

# Co-Simulation of Back-to-Back VSC Transmission System

By

Chathura Jeevantha Patabandi Maddumage

A thesis submitted to the Faculty of Graduate Studies  
at the University of Manitoba  
in partial fulfilment of the requirements for the degree of  
Master of Science

Department of Electrical and Computer Engineering  
Faculty of Engineering  
University of Manitoba  
Winnipeg, Manitoba

August 2011

© Copyright

2011, Patabandi Maddumage Chathura Jeevantha

## Abstract

With the increased complexity of modern power systems, it may be required more than one platform to do an intended study efficiently and accurately. This research was carried out to investigate the use of co-simulation in an application of power system.

A back-to-back Voltage Source Converter (VSC) transmission system was modelled in PSCAD/EMTDC which is an Electro-Magnetic Type (EMT) software. Results were analysed for some operating points of the system.

Then the control system of the above system was modelled in MATLAB/SIMULINK while the rest of the system was modelled in PSCAD/EMTDC. Both of these systems were interfaced to obtain the complete system and results were analysed under same operating points as the original PSCAD case.

# Acknowledgments

This project is carried out at the power system machine lab of the department of Electrical engineering, university of Manitoba, Canada.

First I would like to thank my advisor Prof. S. Filizadeh for his valuable ideas, guidance, encouragement and all other help that he gave me to succeed this work. Also my gratitude goes to all the professors, students and the staff at the power group who help me in numerous ways. I want to express my special gratitude to Dr. M.Heidar and Mr. U. Gnathne for giving me valuable ideas during my difficult times.

My Special thanks go Mr. Erwin Dirks, Mr. Zoran Trajkoski, and all the staff in Tech shop. Many thanks go to my Sri Lankan friends who help me in numerous ways to keep my life in Winnipeg comfortable and enjoyable.

Last but not least, I would like to thanks my parents, my wife, two brothers and all my teachers to help me to achieve where I am today and encouraging me all the time.

Also I would like to thanks Manitoba HVDC centre, MITACS scholarship program, NSERC and University of Manitoba Graduate Fellowship for providing me the financial support to carry out this work.

Chathura J. Patabandi Maddumage

# Dedication

*To my parents and teachers*

# Contents

## Front Matter

Contents .....	iii
List of Tables.....	v
List of Figures .....	vi
List of Symbols.....	ix
List of Appendices.....	xi
<b>1 Introduction</b> .....	<b>1</b>
1.1 Power Electronic Design Using Transient Simulation Tools .....	4
1.2 Motivation and Problem Definition .....	6
1.3 Application Area .....	9
1.4 Thesis Structure .....	9
<b>2 Back-to-Back VSC Transmission System</b> .....	<b>10</b>
2.1 Basic Elements of a Back to Back VSC-HVDC System .....	11
2.1.1 Converter Bridge.....	12
2.1.2 Transformers.....	16
2.1.3 Line Reactor .....	16
2.1.4 AC Filters .....	17
2.1.5 DC Capacitors .....	18
2.2 Pulse Width Modulation (PWM) .....	18
2.2.1 Sinusoidal Pulse Width Modulation (SPWM).....	22

2.3	Operation of VSC-HVDC System.....	25
2.3.1	Control strategy of the VSC .....	27
2.3.2	Continuous-time model.....	28
2.4	Controller Design.....	30
2.4.1	Current Controller .....	30
2.4.2	Outer Loop Controllers .....	31
<b>3</b>	<b>Development of a Simulation Case: Single-Platform Simulation</b>	<b>34</b>
3.1	Electrical System.....	35
3.2	Control System .....	36
3.3	SPWM Generation System.....	38
3.4	Optimization of Control System Parameters .....	40
3.5	Complete System in PSCAD .....	46
3.6	Simulation Results .....	47
<b>4</b>	<b>Co-Simulation of the Test Case</b>	<b>58</b>
4.1	Electrical System in PSCAD/EMTDC .....	60
4.2	Control System in MATLAB/SIMULINK.....	60
4.2.1	Role of the Intermediate m-file .....	60
4.2.2	SIMULINK Control System .....	63
4.2.3	Interfacing to MATLAB/SIMULINK .....	64
4.3	Interfacing Issues .....	66
4.4	Interfacing Benefits.....	68
4.5	Results Comparison.....	69
<b>5</b>	<b>Conclusions and Future works</b>	<b>72</b>
5.1	Conclusions .....	72
5.2	Future works.....	73
	Bibliography.....	75
	Appendices .....	81

# List of Tables

Table 1 : Parameter values of the system in Figure 3-1 [25] [37]. .....	36
Table 2 : Initial values and optimized values of the PI controller parameters of Control system of VSC-A .....	44
Table 3 : Initial values and optimized values of the PI controller parameters of Control system of VSC-B .....	44
Table 4 : No: of simulation runs and time duration for various parts of Objective Function .....	45
Table 5 : Average steady state error % of $V_{dc}$ .....	54
Table 6 : Overshoot of $Q_A$ .....	54
Table 7 : Overshoot of $P_B$ .....	54

# List of Figures

Figure 2-1: Topology of a VSC-HVDC system .....	12
Figure 2-2: Two level VSC Converter Bridge.....	13
Figure 2-3 : Single leg of the Converter Bridge .....	13
Figure 2-4 : Load voltage for a single leg.....	14
Figure 2-5 : Output voltage and the fundamental of it under square wave operation .....	15
Figure 2-6: Waveforms for PWM general case .....	19
Figure 2-7 : Development of Modulation Index.....	21
Figure 2-8: Waveforms for sinusoidal PWM.....	23
Figure 2-9 : Harmonic Spectrum when frequency ratio is 15.....	24
Figure 2-10: VSC model.....	25
Figure 2-11: Single line Diagram .....	26
Figure 2-12: Phasor representation of model 2.8.....	26
Figure 2-13 – dq reference frame.....	27
Figure 2-14: Current Controller .....	31
Figure 2-15: DC Voltage controller .....	32
Figure 2-16: Active power controller .....	32
Figure 2-17: Reactive power controller .....	33
Figure 3-1: Electrical system developed in PSCAD/EMTDC.....	35

Figure 3-2: Control System VSC-A.....	37
Figure 3-3: Control System VSC-B.....	38
Figure 3-4: SPWM generation system.....	39
Figure 3-5 : Basic Interface between optimization and transient simulation [3].....	41
Figure 3-6 : Implementation of the objective function.....	43
Figure 3-7: Block diagram of Optimization system.....	43
Figure 3-8 : Complete system in block diagram form.....	47
Figure 3-9 : Variation of Vdc.....	48
Figure 3-10: Variation of $P_B$ .....	48
Figure 3-11 : Variation of $Q_A$ .....	49
Figure 3-12 : Variation of $Q_B$ .....	49
Figure 3-13: Vdc at dc side of VSC-A.....	50
Figure 3-14: Reactive power (Q) at VSC-A.....	51
Figure 3-15: Active Power (P) at VSC-B.....	52
Figure 3-16: Reactive power (Q) at VSC-B.....	53
Figure 3-17 : Plot of $i_d$ at the VSC_A.....	55
Figure 3-18 : Plot of $i_q$ at the VSC_A.....	56
Figure 3-19: Plot of $i_d$ at the VSC_B.....	56
Figure 3-20 : Plot of $i_q$ at the VSC_B.....	57
Figure 4-1 : Graphical representation of the Integration.....	61
Figure 4-2 : Communication between PSCAD and MATLAB/SIMULINK.....	62
Figure 4-3: Interaction between PSACD and SIMULINK.....	63
Figure 4-4 : Sequence of events in PSCAD to MATLAB interface [1].....	65

Figure 4-5 : Configuration Parameter Dialog box of SIMULINK .....	66
Figure 4-6: Comparison of Vdc .....	69
Figure 4-7: Comparison of Q_A.....	70
Figure 4-8: Comparison of P_B.....	70
Figure 4-9: Comparison of Q_B.....	71

# List of Symbols

$A_c$	- amplitude of the reference signal
$A_r$	- amplitude of the reference signal
AC	- Alternating current
$C_{dc}$	- Capacitor of the dc link
DC	- Direct current
DSP	- Digital signal processing
$f_c$	- frequency of the carrier signal
$f_r$	- frequency of the reference signal
GTO	- Gate turn off
HVDC	- High voltage direct current
IGBT	- Insulated gate bipolar transistor
I/O	- Input output
KVL	- Kirchhoff's voltage law
$m_r$	- Modulation index
OF	- Objective function
$P_{ref}$	- Reference active power
$P_N$	- Nominal apparent power
PI	- Proportional Integral

PLL	- Phase locked loop
PWM	- Pulse width modulation
$Q_{\text{ref}}$	- Reference reactive power
SPWM	- Sinusoidal pulse width modulation
$V_c$	- Voltage at the ac side of the converter
$V_{\text{dc}}$	- Nominal dc voltage
$V_{\text{dcref}}$	- Reference or set dc side voltage
$V_s$	- Grid or source voltage
VSC	- Voltage source converter

# List of Appendices

Appendix 1: Matlab Code for Interfacing PSCAD with MATLAB..... 81

# Chapter 1

## Introduction

In the past few years, there has been significant progress in the development of computer simulation platforms that enable design of power electronic systems by offering facilities such as improved computer models [1] [2], embedded and robust optimization [3], sensitivity and statistical analysis [4], etc. These features that are already implemented in the number of power system transient simulation programs, such as the PSCAD/EMTDC, form a coherent suite of tools that facilitate the design of virtually any system that can be modeled and represented in the simulation environment. This includes complex power electronic (PE) systems with embedded controllers as seen in the emerging power-electronic building blocks (PEBB) [1] [5], detailed model of individual elements such as induction machines, generators, exciters, etc, models of linear and non-linear switching devices, components for doing optimization inside the simulation and multiple run option, [1] [3] [5], etc. Depending on the intended studies one must select which platform needs to be used. Studies such as load flow analysis only require a less detailed model

while short-term high frequency analysis (transient studies) require more detailed models [1].

Modern power systems are large networks interconnecting large geographical areas. For example in the power system in the province of Manitoba, generating stations are located far away from the load centers and there should be an interconnection between these two ends of the system. Also this power system connects to the neighboring provincial networks through transmission lines making a large complex system. In order to do a study of such a system, one may need to use more than one simulation platform, to take advantage of specific modeling and simulation facilities available in each.

This research carries out an investigation on the use of more than one simulation tool to complete a simulation of a power electronic-intensive system. The task of using more than one simulation to complete the simulation of a complex system is often referred to as co-simulation [1]. First the entire system is modeled in a one simulation tool. Next the system is divided into two sections, namely controls and power circuitry, and each is modeled and simulated in a different simulation program. The two simulation tools are interfaced to achieve the complete system operation and investigate the results and potential benefits and problems that may arise when interfacing is done.

Co-simulation has been used for many applications and presented in various references. Use of co-simulation for a complex protection system is presented in [6], where an EMTP type program is used as the simulator for the power system transients while high level language or commercially available software packages such as MATLAB are used to model the protective relays. EMTP TACS – FORTRAN interface development for ad-

vance digital controller is presented in [7]. Reference [8] discussed the interfacing of a real time controller with a digital simulator without relaxation of real-time constraints.

Use of co-simulation between PSCAD and MATLAB/SIMULINK is presented in [9] [10] [11]. The non-linear simplex algorithm written in FORTRAN is interfaced with a transient simulator such as PSCAD, to add the integrated optimization feature for that transient simulator is presented in [3]. Interfacing between PSCAD/EMTDC and the PSB/SIMULINK for the first CIGRE/HVDC benchmark model is presented in [12]. In here, the CIGRE/HVDC benchmark model [13] is modeled in PSCAD/EMTDC and PSB/SIMULINK and interfacing between these two platforms is also considered.

Co-simulation has been done for electronic circuit simulators such as SPICE and SABER as well. DELIGHT.SPICE is a combination of the DELIGHT interactive optimization- based computer-aided-design system and the SPICE circuit analysis program to take the advantage of powerful optimization algorithms [14]. References [15] [16] [17] presented more co-simulation cases for electronic simulators.

This work is carried out as part of a large necessary effort to study a complete design cycle of a power electronic system which starts from computer simulation and ends in transforming it to the actual hardware stage. The research results presented here explain the simulation of the target system, co-simulation and interfacing. Implementation of the actual hardware is not in the scope of the present work.

## 1.1 Power Electronic Design Using Transient Simulation Tools

There is a growing trend towards making modern simulation tools that are design-ready, i.e., they are equipped with facilities that aid the designer in (i) selection of components and topologies, (ii) optimization of the performance of the system, (iii) analysis of the sensitivities involved in design and (iv) analysis of design tradeoffs involved, to name a few [1].

Even though most modern simulators provide these facilities, there is a growing trend to use more than one simulation tool and interface them to obtain enhanced performance and efficiency. Interfacing allows the user to utilise the speciality in different tools to perform a given work with more convenience by taking advantage of particular modeling and simulation abilities of individual programs [1]. The level of co-simulation involved between platforms may vary from simple tasks such as post-processing and visualization of simulation results [9] to complex analysis carried out in a different tool to perform an integral part of the simulation which may require data transfer between platforms at every simulation time step of the simulator program.

While experience confirms that the above facilities have been successfully used in several simulation studies, there is little experience with the complete design cycles involving transition from simulation to actual circuits. Such an experience and in-depth insight have several benefits including:

1. Computer modeling and simulation is only an approximation of the real-world phenomena under consideration; therefore it is important to determine how the simulation results obtained for a given design will perform in real world;
2. Using the outcomes of the above, one can obtain reliable information about what level of details needs to be considered in a simulation-based design. For example, the level of complexity in modeling filtering and measurement elements, impact of delays, and DSP implementation issues can all be quantified;
3. Transition from simulation and computer models to real digital signal processor (DSP)-based controllers is always a challenging exercise. While controller manufacturers often claim transparent and convenient translation, it is frequently observed that the practical transition is not as straightforward. Various types of adjustments and manipulations often need to be done in order to transport a computer simulation model to a DSP-executable control code. These adjustments can potentially lead to changes in the optimized settings obtained through simulation, thus adversely affecting the performance of the final design.
4. Even though co-simulation is tried in many applications due to its benefits discussed above, its true worth and power are yet to be fully understood. If the co-simulation can be applied between different kinds of simulation tools successfully, users may obtain a wide range of benefits that are specific to those tools.

Taking into consideration the above concerns, this research has been undertaken to develop insight into the actual details of the simulation-based design. As an example a

complete design cycle of a power electronic system is targeted to find the answers to the above problems. As a first step, co-simulation is conducted. This allows the designer to confirm accuracy and investigate other simulation aspects such as speed when using more than one simulation program.

## 1.2 Motivation and Problem Definition

As described earlier, it is sometimes necessary to carry out the work of simulation on more than one platform to achieve the final objective of a design or to utilize the built-in analysis/simulation specialties of various simulators. So it is necessary to model the system in two different platforms and interface them using a suitable mechanism.

There are several reasons why one may need to work on more than one platform when analyzing and designing a system as described briefly above. Electric power networks are complex dynamic systems which need various levels of modeling to do different kinds of analysis. The level of detail used to describe the components in one simulation tool may differ from others [1].

When doing a study of a large system, users may need to use specially-designed components in addition to the ones in the component library of the simulation tool. Some tools provide the facility to define user-defined components inside the simulation tool. But sometimes users may need to expand the study to other simulation tools to get the work done more easily and efficiently. The so-called co-simulation is an efficient way of avoiding extensive component development and coding if the required models are available elsewhere [1].

Various kinds of interface and methods are available. Static interfacing, dynamic interfacing and memory management, and wrapper interface are three types of interfacing methods that are discussed in the reference [1]. These interfacing methods may be implemented either as an external interface or an internal interface [1] depending on where it is implemented. If a particular study needs to use more than two simulation platforms, one has to use multiple interfacing techniques, such as core-type interfacing, chain-type interfacing and loop interfacing [1].

In this thesis, interfacing of an EMTP type program with a mathematical tool is discussed. PSCAD/EMTDC is selected as the EMTP type program. This program has detailed models of power system components including power electronic switches. MATLAB/SIMULINK is the selected mathematical type tool. These selections are based on the following facts.

1. PSCAD/EMTDC is widely used software package for power system studies that require short term analysis of complex systems, including power electronic systems which requires detailed time domain modeling of power electronic components. EMTP-type programs, such as EMTDC, are used in applications involving transients that require detailed models. Power electronic systems [1], flexible ac transmission systems [18], high voltage direct current transmission systems [19], over-voltage and insulation co-ordination [20] [21] are a few examples for this [1].
2. MATLAB/SIMULINK is a widely accepted mathematical simulation tool, which is used in different types of analysis. MATLAB allows the user to define and model the components to do large mathematical calculations, provides an easy

and attractive way of visualization, and has special function tool boxes such as optimization tool box, etc. SIMULINK library contains a wide range of components including control system components, power system components, machine models, etc, and allows the user to assemble and simulate a complex system model in a visual manner. Some of MATLAB's toolbox capabilities, such as controls, are well beyond what is available in a typical EMTP-type program and it is developed for the extremely time-coordinating task.

3. SIMULINK also supports and is compatible with other dedicated hardware platforms such as dSpace [22]. MATLAB and SIMULINK include libraries of data acquisition tool box, real time interface libraries and libraries that only support these kinds of hardware platforms. This enables the user to develop models in MATLAB/SIMULINK and connects the model to hardware using this type of dedicated hardware platform. This allows an easy way of prototyping of real systems, which saves cost and money by shortening the cycle of design.
4. Several hardware manufacturers have developed extensive MATLAB/SIMULINK libraries specific for their hardware to allow rapid prototyping and design migration from MATLAB environment to actual hardware [22]. This is a major incentive in linking an EMTP-type program with MATLAB/SIMULINK to allow the use of such facilities

## 1.3 Application Area

A back-to-back voltage-source converter system (described in Chapter 2) is selected as the application example for the demonstration purpose. First this system is completely modelled in PSCAD/EMTDC. Then its control system parameters are optimised using the optimisation tool in PSCAD.

In the next step, only the power circuit is built in PSCAD and rest of the system (control system) is built in MATLAB/SIMULINK. Then these two models are interfaced; the control system developed in SIMULINK is verified to work the same as the one in PSCAD. Investigation on the interfacing and the associated artefacts are presented.

## 1.4 Thesis Structure

The structure of the remaining parts of the thesis is as follows. Chapter 2 gives a brief introduction to back-to-back voltage source converter (VSC) system with its theory, operation details and the control system used in this thesis. Simulation case of the back-to-back VSC transmission system is described in chapter 3. Chapter 4 details the SIMULINK controller design and interfacing of PSCAD and SIMULINK as well as results comparison of pure PSCAD case and interface case. Conclusion and future works are given under Chapter 5.

## Chapter 2

# Back-to-Back VSC Transmission System

Conventionally High Voltage Direct Current (HVDC) transmission is done using thyristor bridge converter systems known as classical HVDC or line-commutated converter (LCC) HVDC systems. Due to the continuous improvement in fully controlled high voltage high power semiconductor devices, an alternative topology based on Voltage Source Converter (VSC), which uses fully controlled semi-conductor devices has become available [23].

Conventional HVDC suffers from communication failure when operated into weak systems; it is also unable to work with loads that have no or insufficient local generation [24]. VSC based systems offer solutions to these cases and as such are gaining popularity in several new installations. Large power system networks depend on the active and reactive power stability. Conventional HVDC systems only allow active power controllability. But with the new VSC based HVDC transmission both active and reactive power can be controlled simultaneously. This means the VSC based systems are more helpful to

achieve stability under faulty conditions. These systems can be used to transfer power in both directions as well depending on the system requirements [25].

As its name suggests VSC transmission is based on voltage-source converters where fully controlled switches are used instead of thyristors which only provide the ON-state control of the switch. The most commonly used type of fully-controlled switches is the Insulated Gate Bipolar Transistor (IGBT) due to its desirable features such as low gate drive requirements, low switching frequency losses, and bidirectional voltage blocking capability [26] [27]. Pulse-Width Modulation (PWM) technologies are used to create the desired voltage waveform with controlled magnitude, phase and frequency. PWM is capable of generating arbitrary waveforms having any phase angle and desired magnitude but it is limited by its switching frequency [26]. Also there are number of PWM technologies available. In this thesis Sinusoidal PWM technique is used. This technique is explained later.

## 2.1 Basic Elements of a Back to Back VSC-HVDC System

Figure 2-1 shows a typical VSC-HVDC transmission system comprising its basic elements. In this system two converters with VSC topology are used where one is used as a rectifier and the other is used as an inverter depending on the direction of the power flow. Other basic elements include line reactors, dc side capacitors, ac system, and dc transmission line.

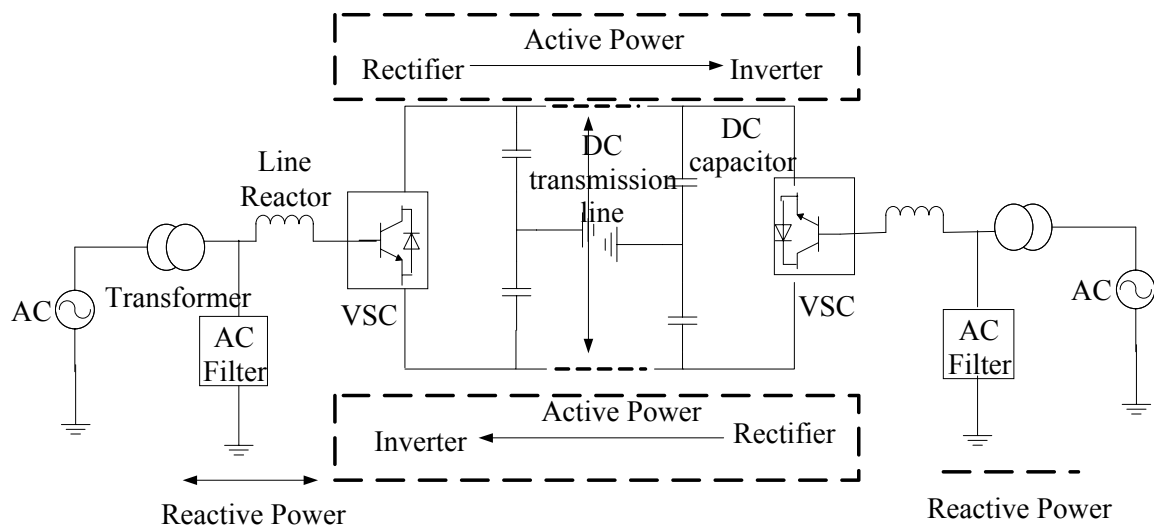


Figure 2-1: Topology of a VSC-HVDC system

### 2.1.1 Converter Bridge

The converter bridge can be realized in many ways depending on the application and the accuracy required for the application. For an example it can be realized as a two level [26], multi-level [28] [29], and modular multi-level converter [30]. The block diagram of a two level three phase six pulse converter bridge, which is used in this thesis, is shown in the Figure 2-2.

As shown in the diagram, the bridge consists of six power semiconductor devices. These devices are fully controlled ones such as Gate-Turn-off Thyristors (GTO) or IGBTs with both turn-on and turn-off capabilities. Anti-parallel diodes are used to maintain full controllability by allowing bi-directional current flow.

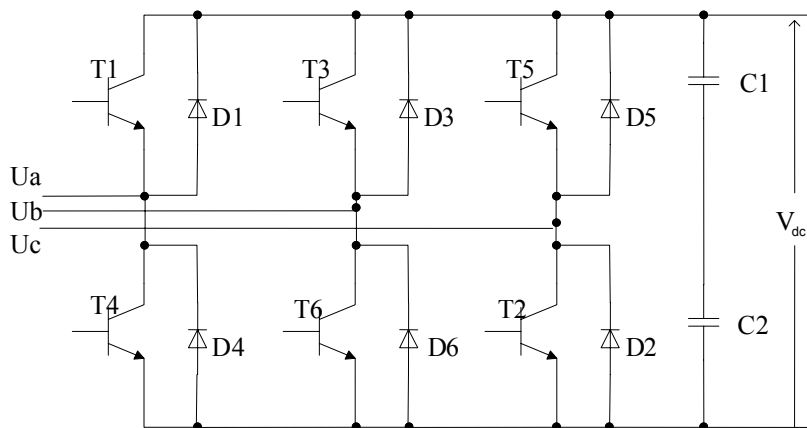


Figure 2-2: Two level VSC Converter Bridge

Consider one leg of the above converter bridge having two dc voltage sources of  $V_{dc}$  each and a resistive load connect at the ac side as shown in Figure 2-3.

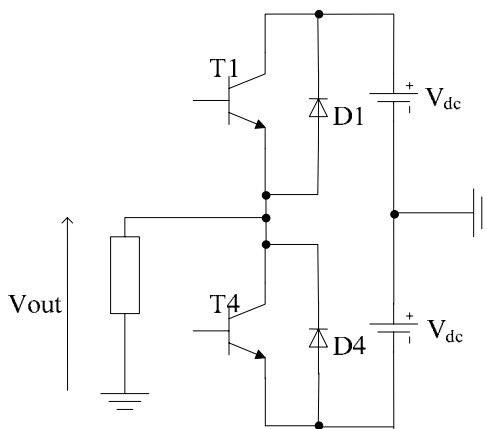


Figure 2-3 : Single leg of the Converter Bridge

When the switch T1 is on while T4 is off, a voltage value of  $V_{dc}$  is applied across the load and when T1 is off and T4 is on,  $-V_{dc}$  is applied across the load. So one can obtain either a  $+V_{dc}$  or a  $-V_{dc}$  voltage level at the load depending on which switch is on and which one is off. This pattern is shown in the figure 2-4. As only two levels are possible in this scheme, it is known as the two levels topology. Note that the switches cannot be

turned ON or OFF simultaneously, as it will cause a short-circuit across the dc source, or interruption of load current, respectively.

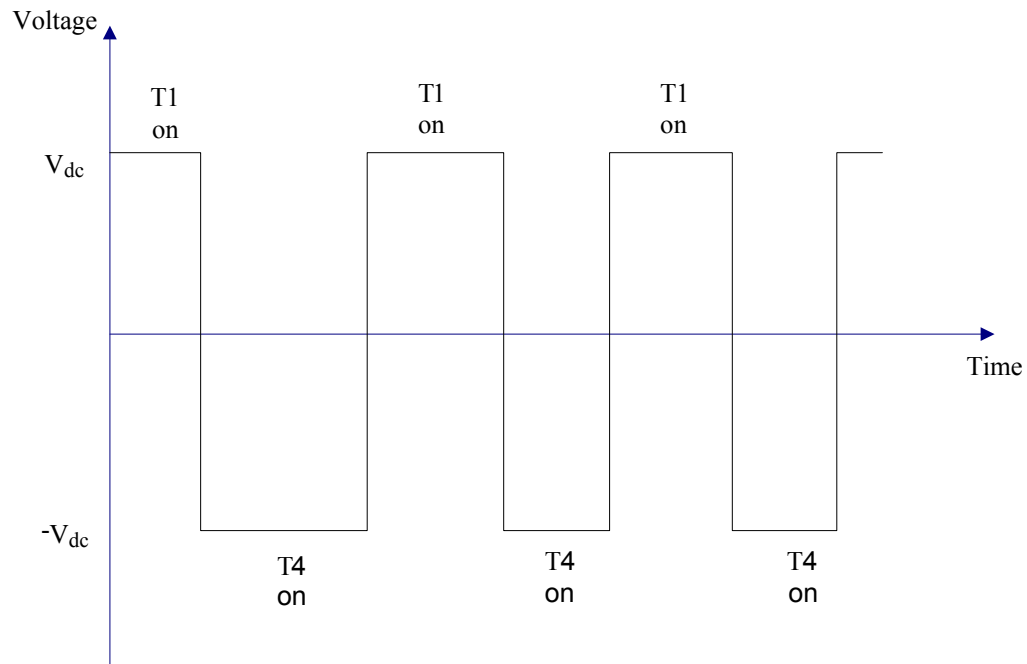


Figure 2-4 : Load voltage for a single leg

If the switches are operated such that each switch conducts 50% of a cycle, the resultant waveform is a square waveform; hence this mode is known as square wave operation. Even though this waveform is not purely sinusoidal, it has a sinusoidal fundamental waveform and a large content of harmonics [26].

Output voltage pulses and its fundamental on the top is shown in the Figure-2.5. As it can be seen from the graph, when the switching frequency is increased, frequency of the pulses is increased and the frequency of the fundamental is also increased.

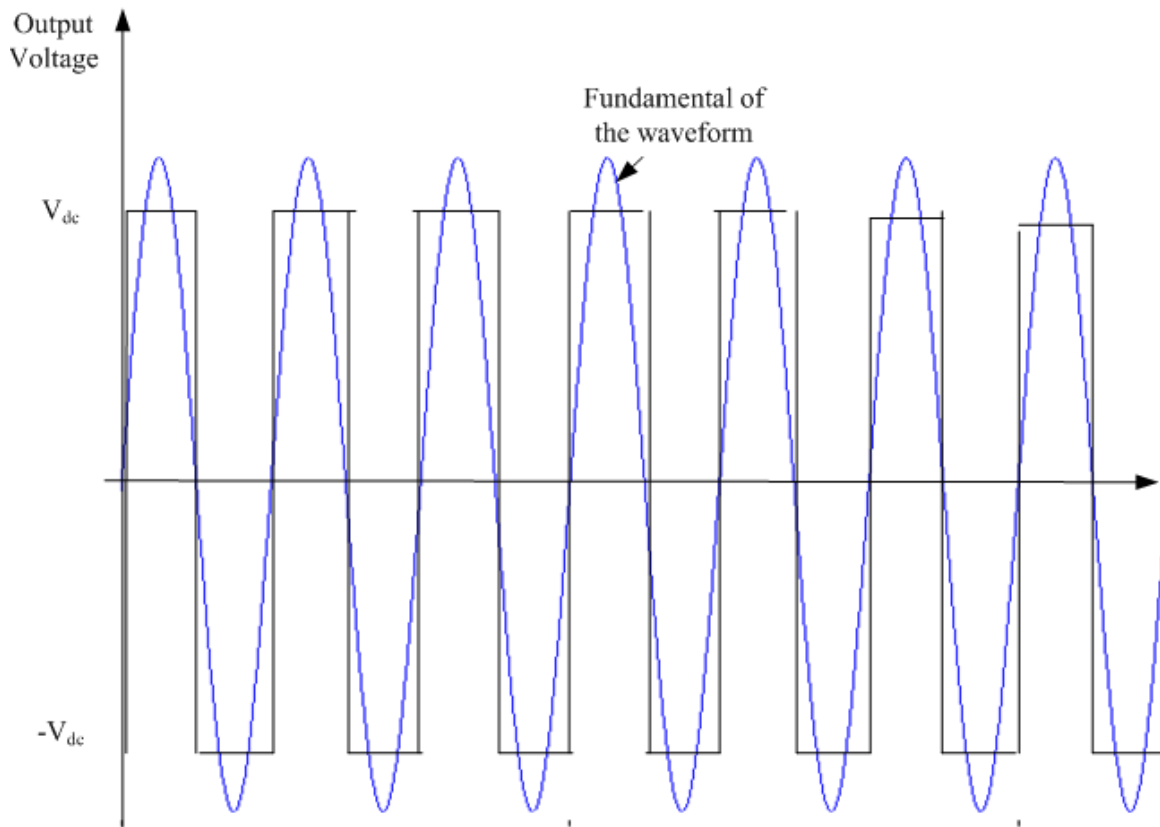


Figure 2-5 : Output voltage and the fundamental of it under square wave operation

This mode does not have a direct controllability over the amplitude of the output voltage unless dc voltage source is changed, which is always not practical. The only variable parameter is the frequency, which can be changed by changing the switching frequency. Also this waveform contains a significant amount of harmonic distortion. The expression for the n-th voltage harmonic is given by [26];

$$V_n = \frac{4V_{dc}}{n\pi} \quad (2.1)$$

It can be seen that the low order harmonics are significant. For example fifth order harmonics is 20 % of the fundamental making filtering difficult and costly. Current har-

monics get damped out due to the inductive nature of the loads resulting in less severe effect. Despite the damping currents harmonic are often not acceptable for practical applications. The n-th order current harmonic is given by [26];

$$I_n = \frac{V_n}{|Z(n)|} \quad (2.2)$$

where  $Z(n)$  is the impedance of the network or load at the n-th harmonic frequency.

So it is necessary to have more advanced techniques such as pulse width modulation techniques (described in section 2.2) to obtain a controllable fundamental, where amplitude, phase and frequency can be changed, and harmonic spectrum can be improved.

### 2.1.2 Transformers

Transformers are used to convert the voltage of the AC system to a value that is acceptable for the converter. This allows the ac voltage value at the ac side of the converter to be at an optimal value considering the ratings of the switches in the converter bridge.

It also provides several other options. Transformer acts as a reactance between the ac system and the converter. It provides the luxury of connecting several VSC systems having different dc voltage levels. Transformers provide a path for the zero sequence components in an unbalance system [24].

### 2.1.3 Line Reactor

Line reactors provide the controllability of active and reactive power flow by varying the current flow across them. The IGBTs in the converter are responsible for generating

higher frequency harmonics which are not suitable for the system. Line reactors also act as a filter to these harmonics.

Depending on user requirements, either a transformer, or a line reactance, or both of them can be used. The following facts have to be considered when designing a line reactance [24].

- Required dynamic behaviour of the system;
- The ac current harmonic content that can flow through the ac system;
- Conditions applied in transient periods and fault situations

#### 2.1.4 AC Filters

Use of power semiconductor devices generates harmonics in the voltage and currents. If these harmonics are transferred to the AC system, they will create severe problems such as improper functioning of equipment, losses, etc. In order to suppress these harmonics, AC filters are employed between the converter and the AC system. In the VSC system lower order harmonics are low due to the use of PWM technique as it removes the lower order harmonics through high frequency switching. This will reduce the amount of filtering required when compared with the traditional thyristor based system [26].

Moreover, filters in LCC-HVDC systems also provide some level of reactive power support that the conductor needs, but VSC-based systems do not require reactive power and hence their filters are typically for low rated [24].

### 2.1.5 DC Capacitors

DC side voltage contains ripples due to the switching action in the converter. DC capacitors are used to reduce this ripple and maintain a steady DC voltage. They provide a path for the turned off current and energy storage, which enables the control of power flow. The value of the capacitor should be selected by considering the voltage on the DC link and also the acceptable ripple value [24].

Equation (2.3) for selecting the capacitor is given in the reference [25].

$$\tau = \frac{0.5 * C_{dc} * V_{dcN}^2}{P_N} \quad (2.3)$$

where  $V_{dcN}$  is the nominal dc voltage and  $P_N$  is the nominal apparent power of the converter.  $\tau$  is the time need to charge the capacitors to the voltage  $V_{dcN}$  if supplied with constant power of  $P_N$  [25].

## 2.2 Pulse Width Modulation (PWM)

As discussed in section 2.1.1., square wave operation does not provide the controllability over the amplitude of the output voltage and also it has a significant harmonic content in the low frequency range. To address these problems waveform synthesis techniques such as PWM are used [26].

PWM is based on the repetitive switching of controlled switches in the bridge of the VSC to produce positive or negative voltage pulses. Durations of these pulses are varied to generate the desired fundamental and reduce the impact of harmonics by pushing the

lower order harmonics as far as possible to higher frequency ranges. These harmonics may contain both odd and even ones. By selecting proper techniques, one can eliminate certain harmonics. Quarter-cycle symmetry is a fundamental property where the waveform can be fully represented using the information in only a quarter cycle of the period of the waveform. This property helps to eliminate the even-ordered harmonics present in the waveforms. Therefore all PWM techniques are designed to ensure that the resulting waveform has quarter-cycle symmetry [26] [27].

Numerous PWM generation methods are available in literature such as sinusoidal PWM, selective harmonic elimination, etc [26] [27]. In this thesis Sinusoidal PWM (SPWM) is used and is explained under section 2.2.1.

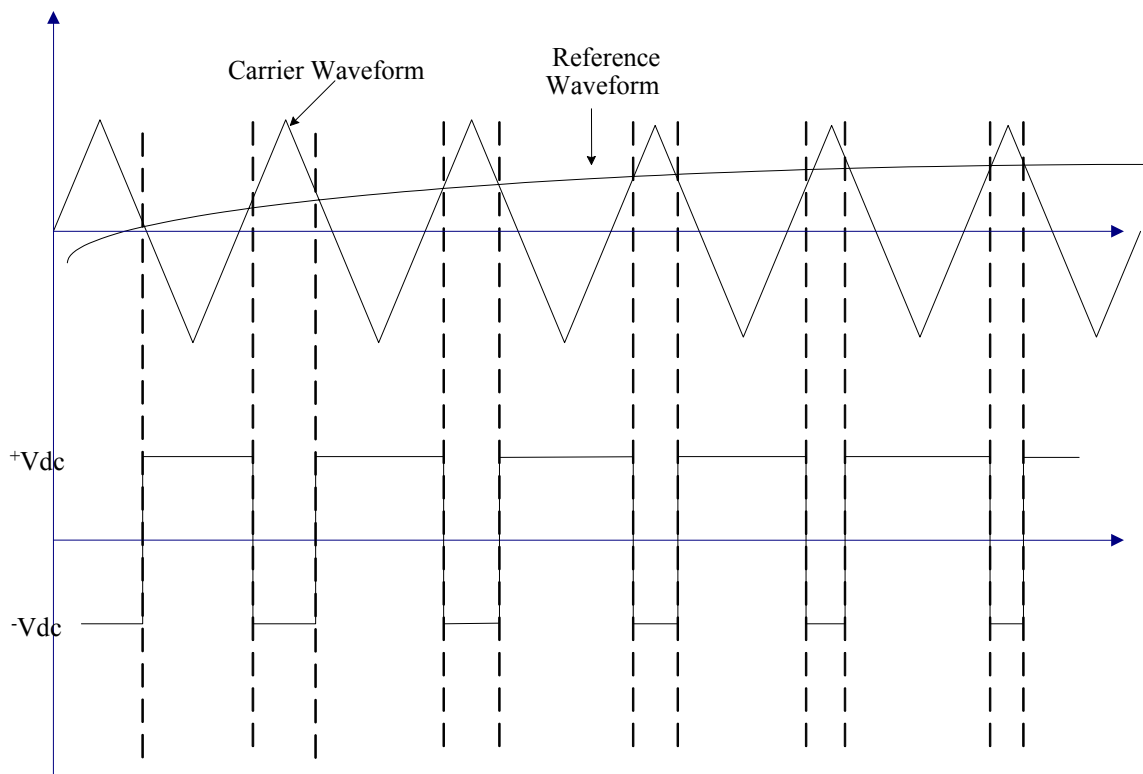


Figure 2-6: Waveforms for PWM general case

Generation of waveforms under PWM is based on the comparison of a high frequency triangular carrier waveform with a low frequency reference waveform, which is produced by the control system. The type of reference signals may vary depending upon the type of PWM method used. The waveforms for a general case are shown in Figure 2-6 where the reference signal is a slowly varying waveform compared with the triangular carrier waveform.

Switching rule is given by following relationship [26];

$$\text{Switch} = \begin{cases} \text{ON} & \text{if carrier} < \text{ref} \\ \text{OFF} & \text{if carrier} > \text{ref} \end{cases}$$

When the reference waveform is larger than the carrier, the switch is on, which results in a positive voltage at the output and vice versa. With a switching frequency sufficiently high, the harmonics are shifted away from the lower order band, which results in better quality waveforms. However higher switching frequency means more switching losses. So one needs to make a compromise between the switching frequency and the harmonic spectrum.

Consider the case shown in Figure 2-7, of having a high frequency carrier waveform with period  $T_c$  which is much smaller than the smallest time constant of the system. As described above output voltage is obtained by comparing this high frequency carrier waveform with the reference waveform having the same switching rule as above.

The dc value or the average value of the output voltage can be obtained by the following equation [26].

$$\frac{(x_2 - x_1)V_{dc} + (x_1 + (T_c - x_2))(-V_{dc})}{T_c} = m_r V_{dc} \quad (2.4)$$

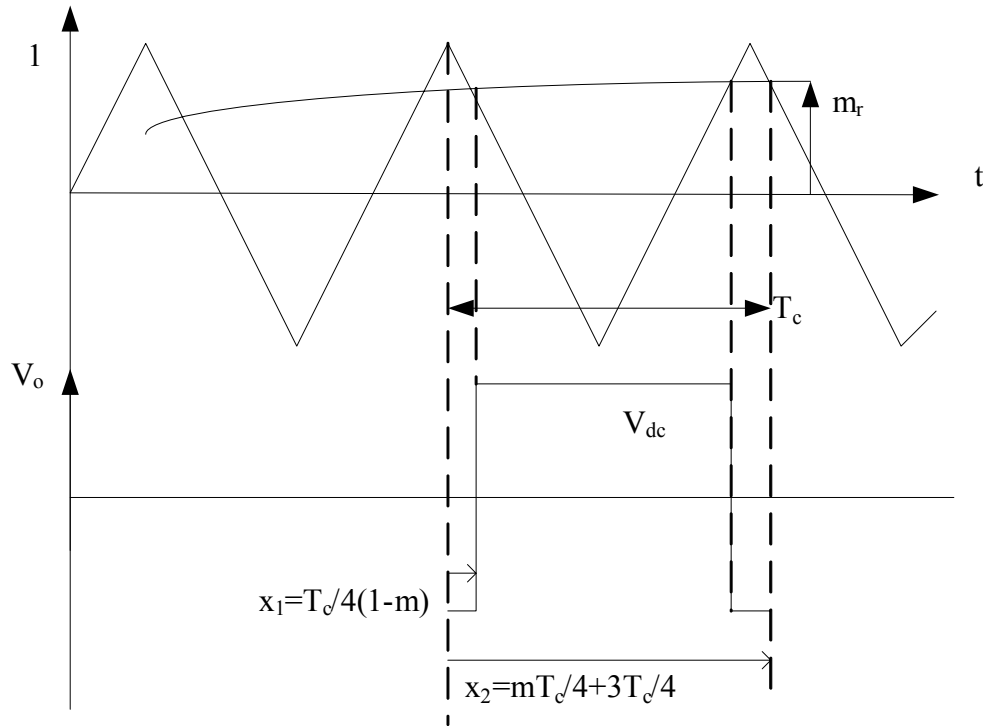


Figure 2-7 : Development of Modulation Index

This means the moving dc value (average value) over a carrier period of the output voltage is directly proportional to the local amplitude of the reference waveform.

$$\langle V_{out} \rangle_T = m_r \cdot V_{dc} \quad (2.5)$$

This proportional constant is defined as the modulation index  $m_r$  [26].

Also the ratio between the frequencies of carrier waveform  $f_c$  and the reference waveform  $f_r$  is defined as the frequency ratio  $m_f$  of the system [26].

$$m_f = \frac{f_c}{f_r} \quad (2.6)$$

The output waveform has a fundamental frequency that equals to the reference waveform frequency and it contains other harmonics depending on the employed PWM method and the frequency ratio between two waveforms. If the reference waveform is a slowly varying one, the average output voltage in a given switching cycle is the same as the reference signal.

### 2.2.1 Sinusoidal Pulse Width Modulation (SPWM)

In SPWM, the modulating signal is a slowly varying sinusoidal signal with the above switching rule. The sinusoidal waveform has quarter cycle symmetry, which manifests itself in the output waveform as well. The waveforms for a SPWM are given under Figure 2-8 with a triangular carrier and the gate signals are produced by the above switching rule.

It can be shown that the modulation index ( $m_r$ ) is  $A_r/A_c$  [26] and frequency ratio is  $f_c/f_r$  [26] where  $A_r$  and  $A_c$  are the amplitude of reference and carrier respectively and  $f_c$  and  $f_r$  are frequency of carrier and reference respectively. To ensure quarter cycle symmetry in the output, one needs to select the frequency ratio as an odd integer. Since 3<sup>rd</sup> order harmonics do not cause problems in balanced three phase situation, they will be eliminated for line quantities, this integer is selected to be an odd multiple of 3 [26].

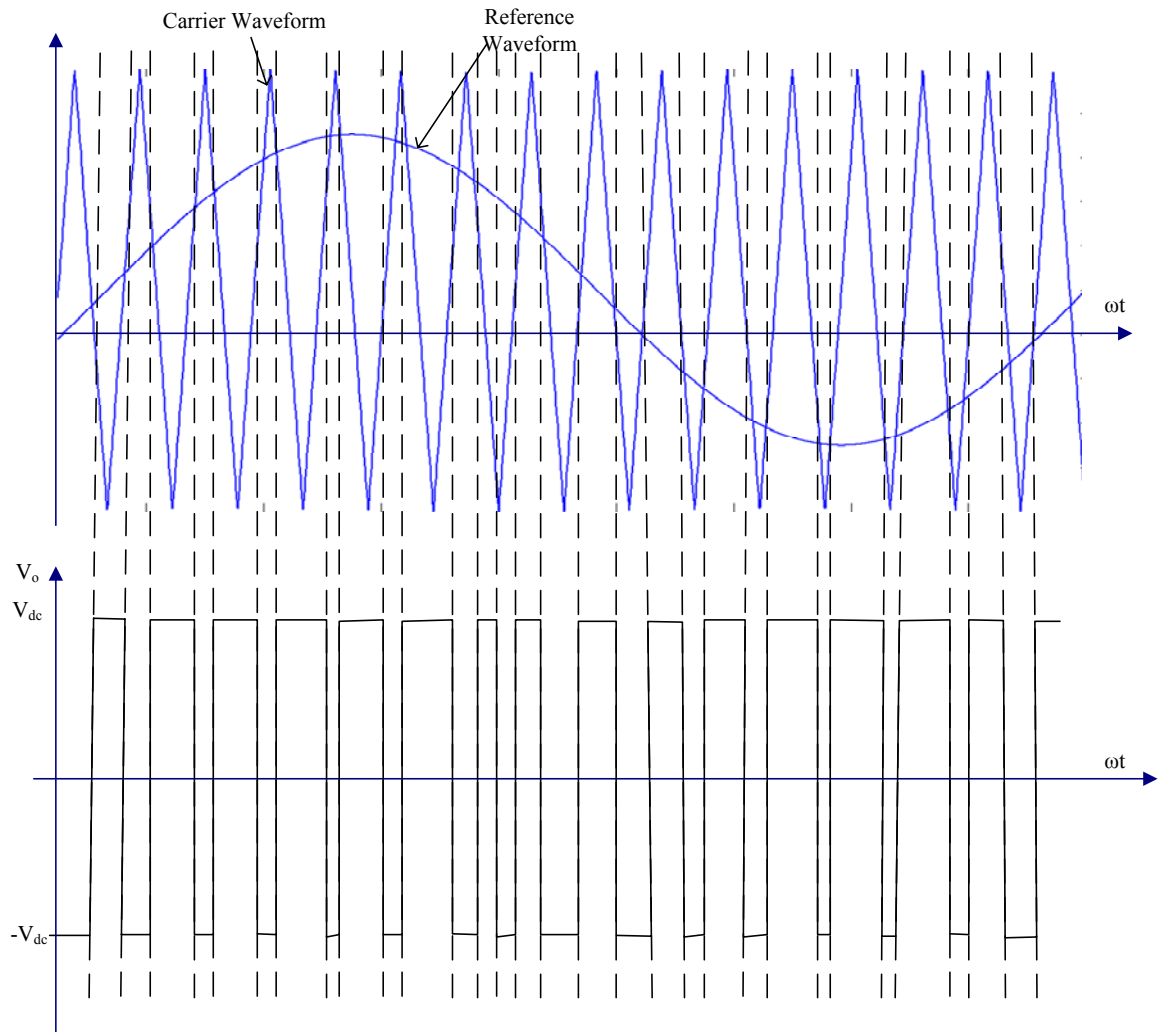


Figure 2-8: Waveforms for sinusoidal PWM

This scheme produces output voltage waveforms with much less low-order harmonic spectrum. For example if the frequency ratio is selected to be 15, then the harmonic order can be obtained as in Figure 2-8. As the ratio is selected to be as an odd integer all even-order harmonics disappear while the other harmonic content will be concentrated more around 15, 30, and other multiples of 15. Due to the inductive nature of the loads, currents harmonics are less significant when the voltage harmonics are at higher frequency

range. The modulation index of the converter is equal to 0.8 for the spectrum in Figure 2-9.

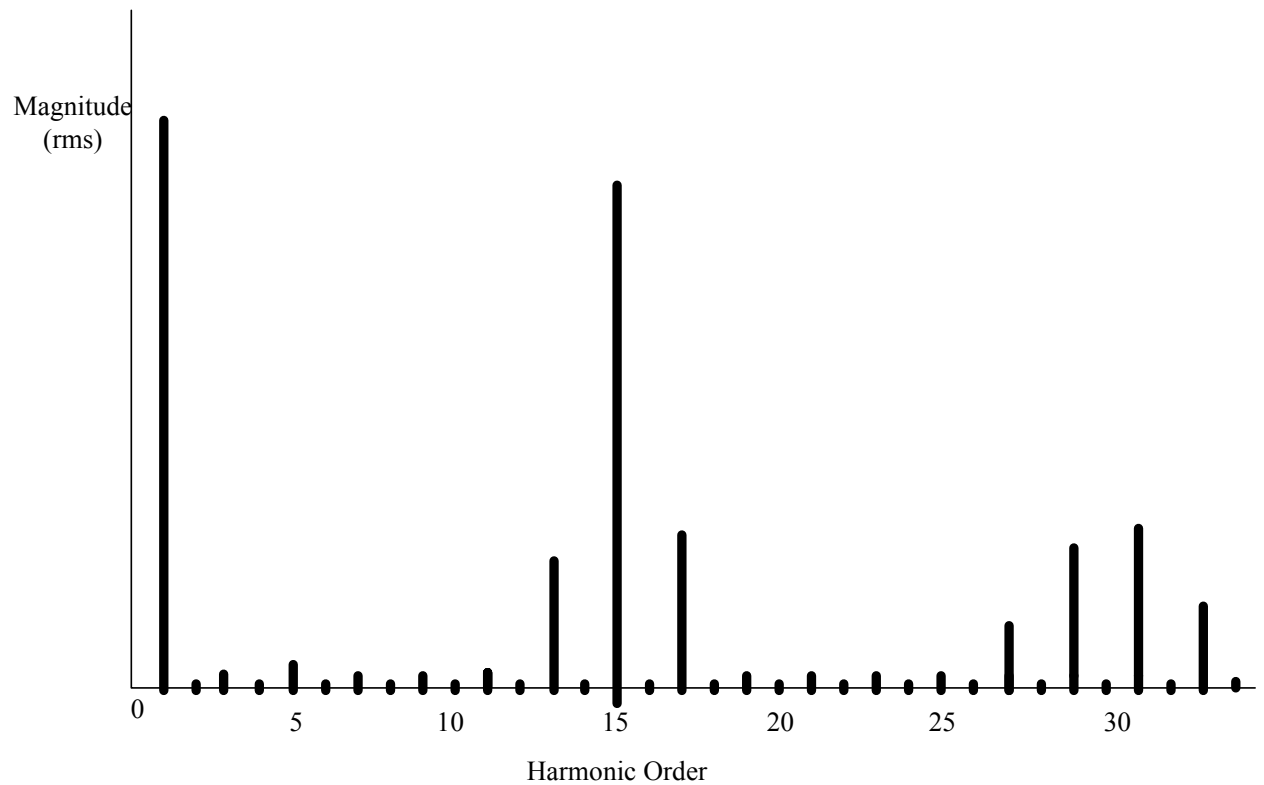


Figure 2-9 : Harmonic Spectrum when frequency ratio is 15

In SPWM, when the modulation index is between 0 and 1, it has a linear relationship with the fundamental; while it is larger than 1, the relationship becomes non-linear. When it is by far larger than unity, it approaches the saturation operation. It is therefore recommended that operation over unity modulation index to be avoided.

## 2.3 Operation of VSC-HVDC System

As mentioned before a VSC consists of either IGBTs or GTOs operated under a PWM technique. The model shown in Figure 2-10 is used in this thesis for the analysis purpose and the following analysis is as presented in [31] where the VSC is considered as a linear power amplifier without considering the detailed nature of the converter [32]. Based on this assumption, a simple model is developed to be used in power system studies [33].

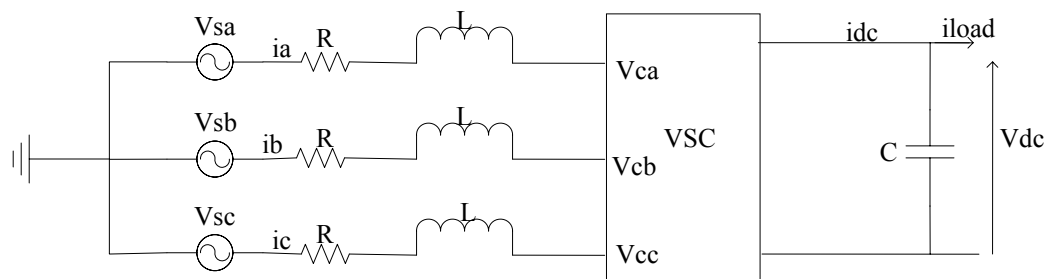


Figure 2-10: VSC model

The converter can be considered as a variable voltage source whose amplitude, phase and the frequency can be controlled independently. Depending on the gate pulses, which are generated by a PWM method, one can change the value of the voltage easily. The amplitude of the output voltage can be controlled by the amplitude of the reference waveform (or the modulation index). Frequency of the output can be changed by varying the frequency of the reference signal.

With the assumptions, the voltage-source converter can be approximated as a fundamental frequency sinusoidal source with controlled parameters. Single line diagram and

the phasor representation of this model are shown in the figures 2-11 and 2-12 respectively [31].

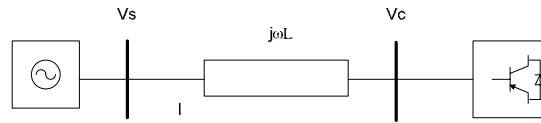


Figure 2-11: Single line Diagram

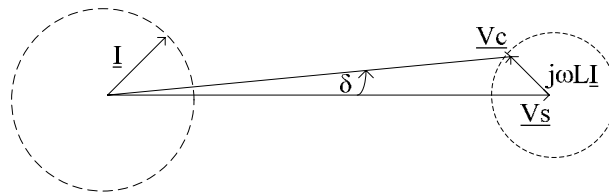


Figure 2-12: Phasor representation of model 2.8

Ignoring the harmonics, the voltage at the AC side of the converter is given by the phasor  $\underline{V}_c = V_c e^{j\delta}$ , which leads the  $V_s$  (grid or source voltage) by the angle  $\delta$ . Based on this the active and reactive power flow can be represented by the following well known formulas [31].

$$P = \frac{V_s V_c}{\omega L} \sin \delta \quad (2.7)$$

$$Q = \frac{V_s (V_s - V_c \cos \delta)}{\omega L} \quad (2.8)$$

It can be seen from the above two equations that the power flow between ac and dc can be controlled by adjusting  $V_c$  and  $\delta$ . It is further observed that the P and Q are coupled in the sense that any change in either  $V_c$  or  $\delta$  will affect both P and Q simultaneously.

### 2.3.1 Control strategy of the VSC

Various controlling methods for VSC are available in references. Direct Power Control (DPC) [34] is such a method, which is based on direct active and reactive power control of the converter. This method does not need a PWM technique and it is based on switching table, which is based on the error between the reference and actual values of active and reactive power. This method has disadvantages such as need of fast conversion and computations, and hence it is not common [35].

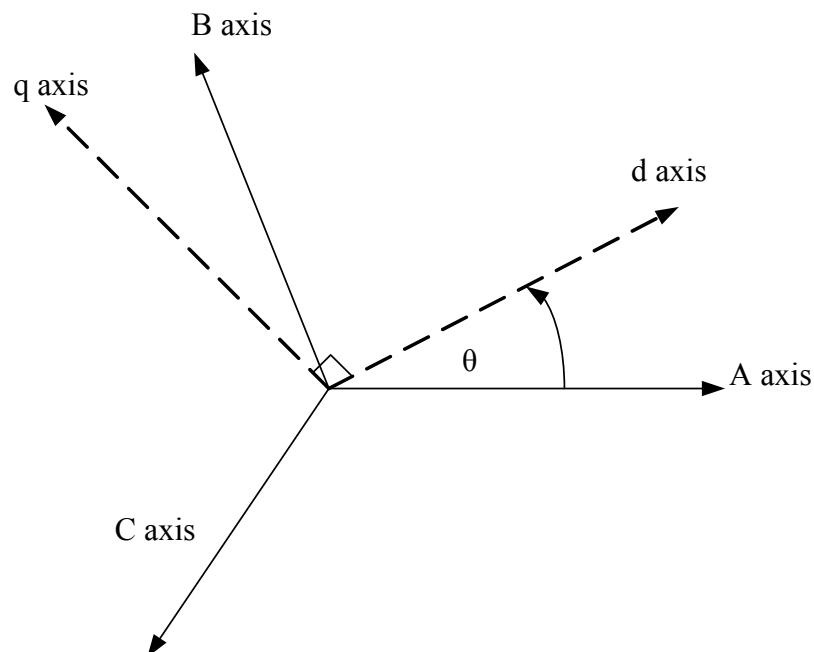


Figure 2-13 – dq reference frame

Vector control strategy is another method that is widely used [31]. It is based on current control strategy in dq reference frame and is used in this thesis. This method transforms the three phase quantities to a different coordinate system known as dq frame as shown in Figure 2-13. In this reference frame, under steady state, currents and voltage vectors acts like constants. As a result of this, pi controllers can be used to eliminate the

static errors in the control system [35]. Also this scheme helps to control the active and reactive power independently.

The following section describe the formulation of equation for the operation of VSC considering it as a linear amplifier first in time domain and next in dq reference frame by applying Park's transformation.

### 2.3.2 Continuous-time model

Consider the idealized VSC shown in Figure 2.10 to derive the equations in the time domain. By applying KVL (Kirchhoff's Voltage Law) for three phases separately, one can obtain the following three equations. The resistance, R represent the line resistance and resistance of other elements between the source and the converter.

$$\begin{aligned}
 V_{sa} - Ri_a - L \frac{di_a}{dt} - V_{ca} &= 0 \\
 V_{sb} - Ri_b - L \frac{di_b}{dt} - V_{cb} &= 0 \\
 V_{sc} - Ri_c - L \frac{di_c}{dt} - V_{cc} &= 0
 \end{aligned} \tag{2.9}$$

Applying Park transformation which is given by,

$$P = \begin{bmatrix} \cos \theta & \cos(\theta - 120) & \cos(\theta - 240) \\ \sin \theta & \sin(\theta - 120) & \sin(\theta - 240) \\ \frac{1}{2} & \frac{1}{2} & \frac{1}{2} \end{bmatrix} \tag{2.10}$$

Yields;

$$V_{dq0} = P.V_{abc}$$

With  $\theta=\omega t$ , (2.9) can be re-written as below after applying (2.10)

$$\begin{aligned} V_{so} - Ri_o - L \frac{di_o}{dt} - V_{co} &= 0 \\ V_{sd} - Ri_d - L \frac{di_d}{dt} - \omega Li_q - V_{cd} &= 0 \\ V_{sq} - Ri_q - L \frac{di_q}{dt} + \omega Li_d - V_{cq} &= 0 \end{aligned} \quad (2.11)$$

In this thesis only a balanced three phase system, which does not induce any zero sequence components, is considered. Hence the zero sequence components are neglected.

The active power at the ac side can be represented in the dq reference frame as in (2.11) after applying the park transformation to the three phase power equation [31];

$$P_{ac} = V_{cd} \times i_{cd} + V_{cq} \times i_{cq} \quad (2.12)$$

Assuming a lossless converter, power balance must hold as follows;

$$P_{ac} = P_{dc} = V_{dc} \times i_{dc} \quad (2.13)$$

From 2.12 and 2.13,

$$i_{dc} = \frac{V_{cd} \times i_{cd} + V_{cq} \times i_{cq}}{V_{dc}} \quad (2.14)$$

At the DC side one can obtain the current and voltage relationship as below.

$$i_{load} = i_{dc} - C \frac{dV_c}{dt} \quad (2.15)$$

By selecting  $i_q$ ,  $i_d$  and  $V_{dc}$  as state variables, the state space representation of the system can be deduced as in 2.16.

$$\begin{aligned}
L \frac{di_d}{dt} &= V_{sd} - Ri_d - \omega Li_q - V_{cd} \\
L \frac{di_q}{dt} &= V_{sq} - Ri_q + \omega Li_d - V_{cq} \\
C \frac{dV_{dc}}{dt} &= \frac{V_{cd} \times i_{cd} + V_{cq} \times i_{cq}}{V_{dc}} - i_{load}
\end{aligned} \tag{2.16}$$

It can be seen that by treating  $\omega Li_x$  term as a disturbance,  $i_d$  and  $i_q$  can be decoupled which results in a decoupled control system as described next.

## 2.4 Controller Design

Control system can be divided into two parts as inner current controller and the outer loop controller. Formation of these two controllers is described next.

### 2.4.1 Current Controller

By introducing two new terms  $x_d$  and  $x_q$  to the first two equations in (2.16) with the assumption of resistance being negligible, the following two equations (2.17) which are a representation of two independent first order models as in (2.18), can be derived [31].

$$\begin{aligned}
x_d &= V_{sd} - \omega Li_q - V_{cd} \\
x_q &= V_{sq} - \omega Li_d - V_{cq}
\end{aligned} \tag{2.17}$$

$$x_d = (sL + R)i_d \tag{2.18}$$

$$x_q = (sL + R)i_q$$

The equations in (2.18) are identical to each other hence a pair of identical control systems to control  $x_d$  and  $x_q$  as shown in Figure 2-14 can be obtained. Outer loop controllers described below generate the current reference values. The developed control system regulates the currents  $i_d$  and  $i_q$  to follow the reference values [31].

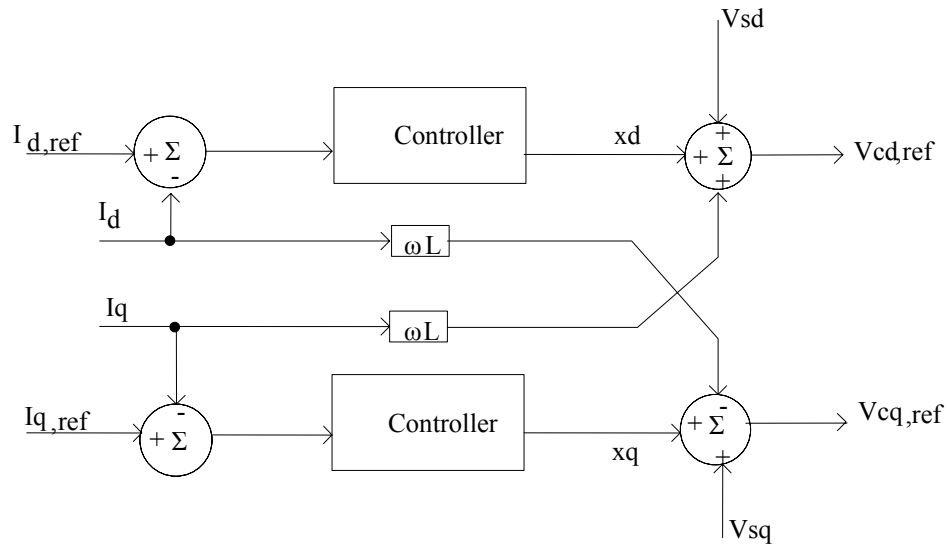


Figure 2-14: Current Controller

### 2.4.2 Outer Loop Controllers

The currents  $i_q$  and  $i_d$  can be independently controlled as shown in (2.17) and (2.18).

Hence the VSC is able to perform two independent control modes at the same time.

- DC voltage control, frequency control or active power control

This mode of operation provides the  $i_{q,ref}$  to the current controllers.

- Reactive power control or ac-voltage control

This mode of operation provides the  $i_{d,ref}$  to the current controllers.

In this thesis, left hand side VSC (VSC-A) operates in DC voltage control mode (generates  $i_{q, \text{ref}}$ ) and reactive power (generates  $i_{d, \text{ref}}$ ) control mode while right hand side VSC (VSC-B) operates under active power (generates  $i_{q, \text{ref}}$ ) and reactive power (generates  $i_{d, \text{ref}}$ ) control modes. Other control modes may also be employed depending upon user requirements [31] [36] [37].

DC voltage controller is implemented by a proportional-integral (PI) controller as given in Figure 2-15 which minimises the error between the reference dc side voltage and actual measurement value of the dc bus voltage.

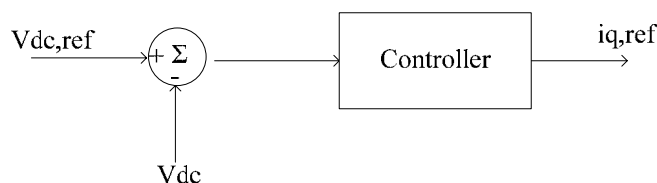


Figure 2-15: DC Voltage controller

Active power (Figure 2-16) and reactive power (Figure 2-17) controllers have similar arrangements where voltages are replaced by either active or reactive power. By controlling active power and dc voltage of two sides of the VSC, the constant dc voltage at the dc side is maintained.

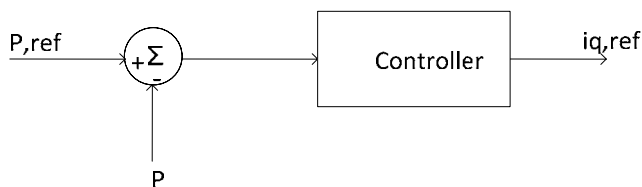


Figure 2-16: Active power controller

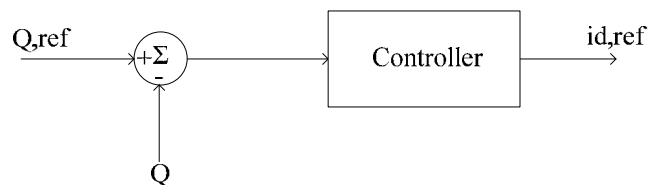


Figure 2-17: Reactive power controller

Outer loop controllers and inner loop controllers are combined to form the full control system. VSC\_A is based on dc voltage and reactive power control modes. Hence control systems represent in Figure 2.15 and Figure 2.17 combined with the inner current controller in Figure 2-14 to form the control system in VSC\_A. Similarly control systems in Figure 2-16 and Figure 2-17 are combined with the current controller to make the control system of VSC\_B as it operates in active power and reactive power control modes. This developed model of the VSC for a back-to-back VSC transmission system is applied and described in the Chapter 3.

## Chapter 3

### Development of a Simulation Case:

### Single-Platform Simulation

The back-to-back VSC system described in chapter 2 is modelled in the PSCAD/EMTDC transient simulator. PSCAD/EMTDC is a widely used software package for power system simulation studies as it has detailed models of components, which make it a benchmark for other models developed using less detailed data. The models developed using analysis, such as small signal stability analysis which only focus on linearising data around an operating point and do not consider the high frequency oscillations in the system, are validated using the results obtained by modelling the same system in PSCAD/EMTD [38]. Hence the results obtained from PSCAD can be considered as a benchmark for the comparison of results obtained from other methods.

As the system is intended to be built on hardware, power ratings of the system is selected to be such that they can be implemented under laboratory conditions considering the implementation aspects. The selected power rating for this case is 1 kW as it allows

using of an existing converter, PS11015, which is available in the lab. Simulation results are obtained for different operating points.

### 3.1 Electrical System

The electrical system of the back-to-back VSC system, which is modeled in PSCAD/EMTDC, is shown in Figure 3.1. In this system, only the ac system, line reactors, converter and dc capacitor are used. AC side filters are neglected as the two ac sides have two three phase electrical sources and also use of sinusoidal PWM technique in VSC eliminates the low order harmonics. However in practical systems high-pass filters are employed to remove the higher order harmonics present in the waveforms. A Phase locked loop (PLL) is used to lock out the phases of the ac system, which is needed when transforming the time domain quantities of voltage and currents to dqo reference frame as described in Section 2.3. It also serves to provide the reference phase angle for the pulse-width modulation scheme.

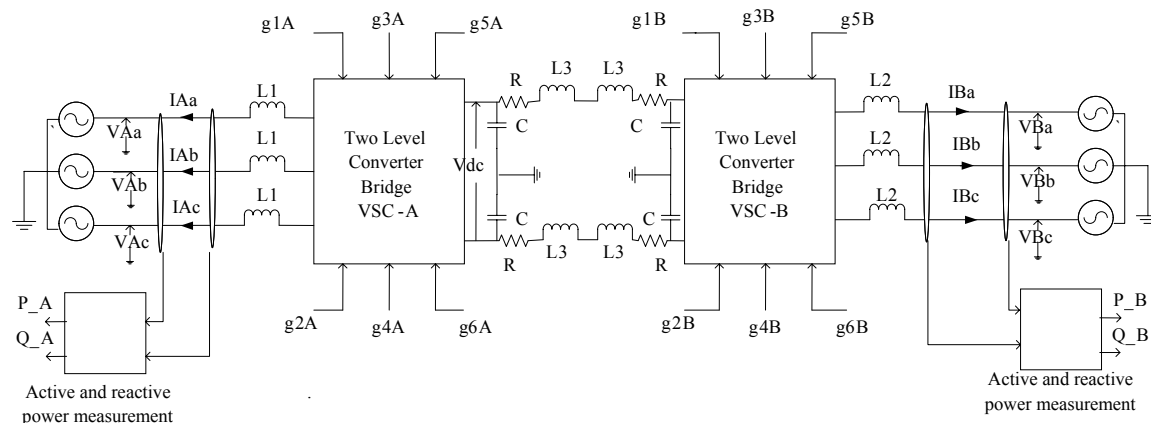


Figure 3-1: Electrical system developed in PSCAD/EMTDC

---

The parameters of the system are calculated as described in section 2.2 and listed in the Table 1.

Table 1 : Parameter values of the system in Figure 3-1 [25] [37].

Parameter	$L_1$	$L_2$	$L_3$	$C$	$R$
Value	0.02 H	0.01 H	0.001 H	50 $\mu$ F	1 $\Omega$

## 3.2 Control System

The controller is designed as described in Section 2.4. Both outer loop controller and current controller are combined to develop the reference waveform of the sinusoidal PWM. The left hand side converter (VSC-A) has dc voltage and reactive power control modes (Figure 3-2) while the right hand side converter (VSC-B) has active power and reactive power control modes (Figure 3-3). The abc-dq0 and dq0-abc blocks available in PSCAD are directly used to transfer quantities between two reference frames.

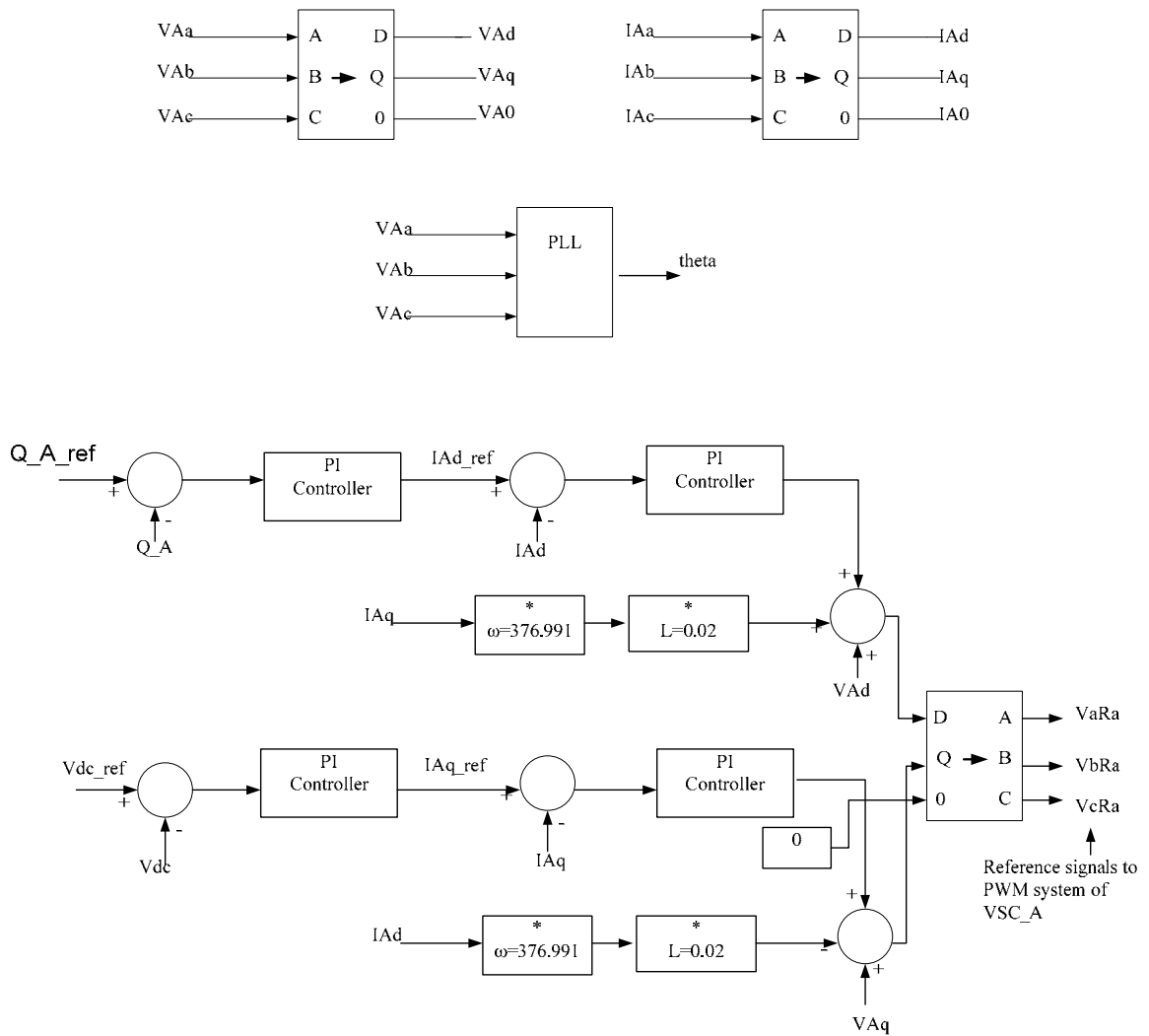


Figure 3-2: Control System VSC-A

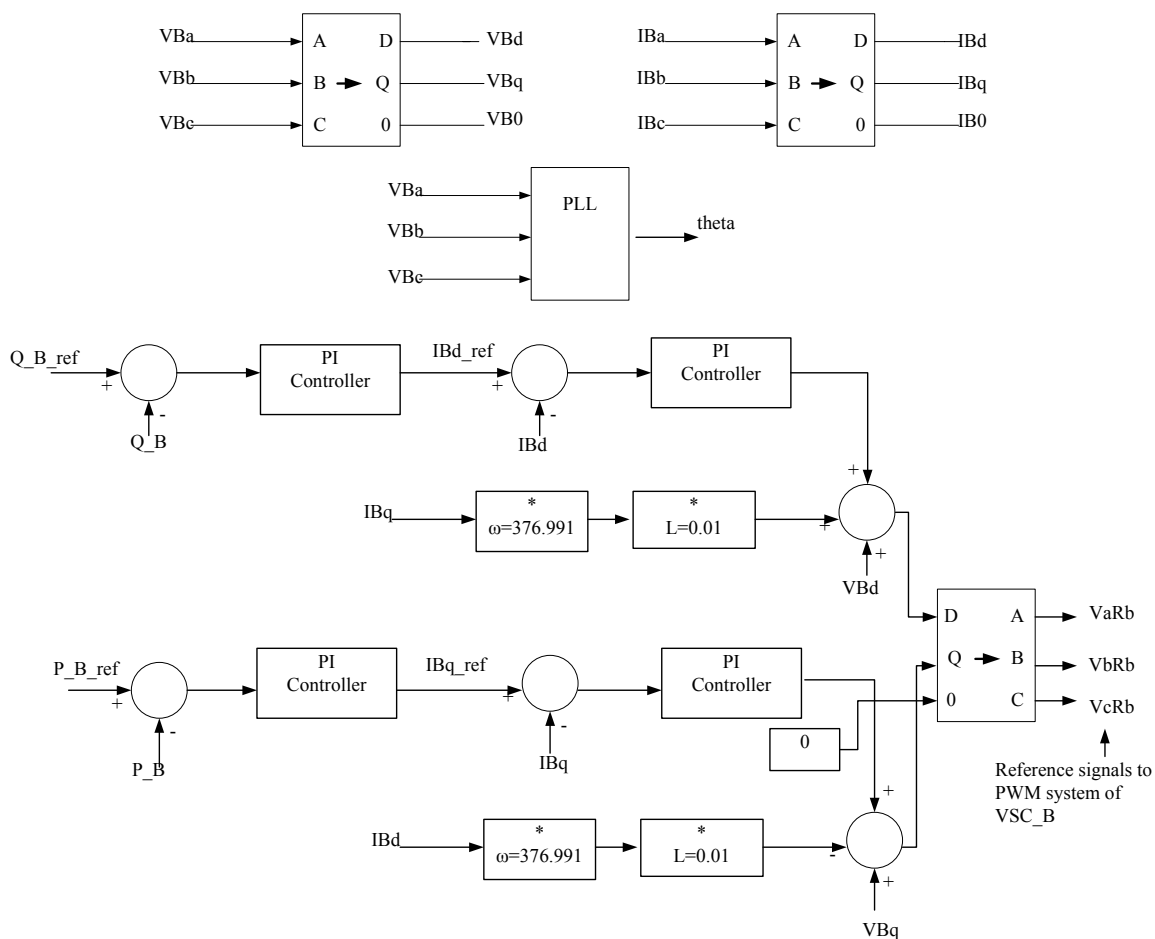


Figure 3-3: Control System VSC-B

### 3.3 SPWM Generation System

As mentioned earlier, SPWM is employed to generate the gate signals of the controlled switches in the bridge. Reference waveforms are obtained from the control system described in Section 3.2 and used a triangular carrier waveform having frequency 1980 Hz which gives frequency ratio of 33. Reference waveforms are multiplied by a constant fac-

tor to bring the reference waveform to a value closer to 0.8 of carrier amplitude to obtain a modulation index of 0.8 when operating under normal conditions. By selecting modulation index on this region, additional room, i.e. [0.8, 1.0] is left for control operation in the linear range. Then these two waveforms are fed to the comparator block in PSCAD as depicted in Figure 3-4 to generate the gate signals of the IGBTs.

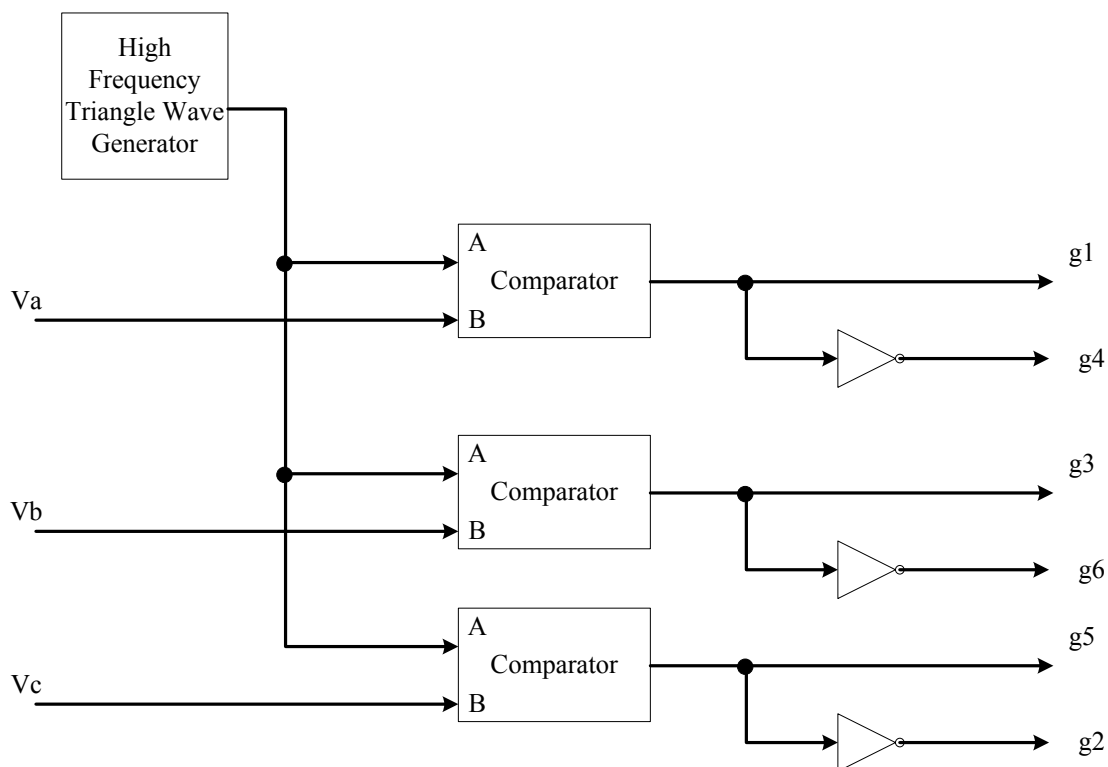


Figure 3-4: SPWM generation system

---

## 3.4 Optimization of Control System Parameters

In the control system developed under Section 3.2, eight Proportional-Integral (PI) controllers are used in inner current controllers and outer current controllers at the two VSCs.

The transfer function of the PI controller is given by the following equation.

$$PI(s) = K_p + K_i / s \quad (3.1)$$

As can be seen from the equation, PI controllers have two parameters, namely proportional gain ( $k_p$ ) and integral gain ( $k_i$ ). To get a proper response, these parameters need to be tuned. Numerical methods such as zero-pole placement method, Z-N method [39], etc are available for the tuning of these parameters. Use of these analytical methods in power systems is difficult as it is complex, non-linear and large.

Hence optimization based algorithms are used to tune the parameters in the PI controllers. Most of these optimization algorithms such as Newton's method [40] need a well defined objective function for the implementation of the algorithm. As the power system has a complex dynamic behaviour, it is difficult to form a well defined objective function [3]. However some optimization algorithms such as Nelder-Mead Simplex method [40], does not need an explicit well defined objective function, hence can be used in a black-box optimization fashion [3] [5].

The algorithm inside the optimization block of the PSCAD/EMTDC can be represented using the block diagram in Figure 3-5. First some initialization values or operating points for the parameters need to be decided. This can be done using a trial and error method. Then these are used to evaluate the objective function value, which is formed inside the transient simulator (PSCAD/EMTDC in this case), of the optimization algorithm.

Formulation of objective function for this case is discussed below. After that, the objective function value for the initial case is compared with the algorithm termination criteria. If this criterion is not satisfied, the next values of the parameters are calculated using the optimization algorithm based on the previous values. This process is continued until the termination criterion is satisfied. If the termination criterion is satisfied, then algorithm stops and produces the optimized values of the parameters [3].

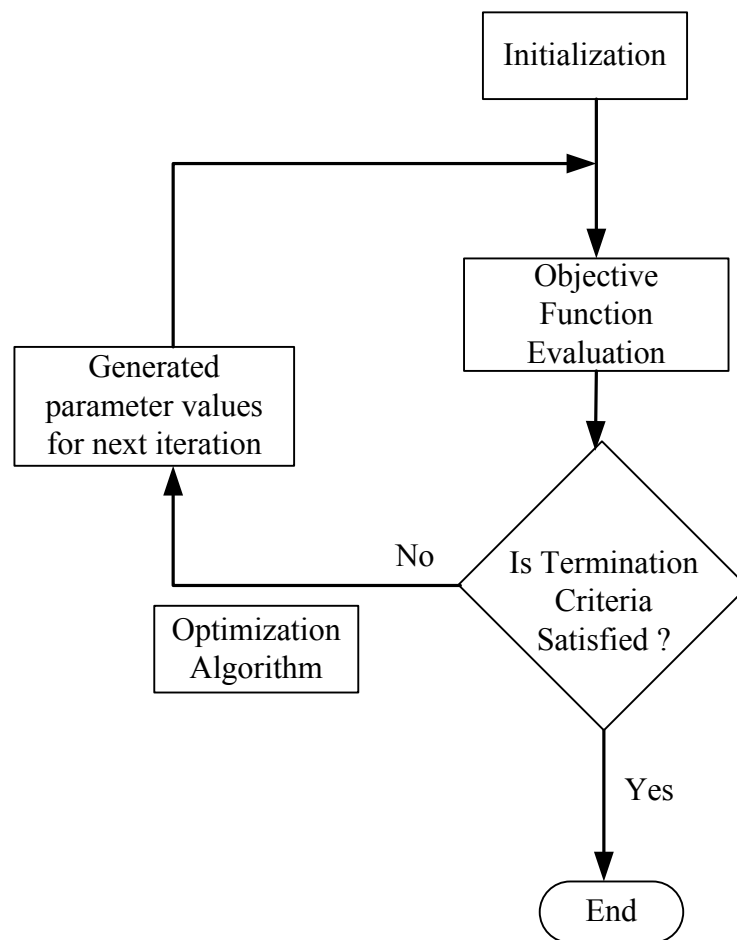


Figure 3-5 : Basic Interface between optimization and transient simulation [3]

The initial values that are obtained using trial and error method are used to obtain a stable operating point to start the optimization process. If these initial values are selected properly, i.e. if they are close to optimal point, the number of simulation runs needed to achieve the optimization is low. As mentioned above, optimization block of the PSCAD/EMTDC is used to optimize the operating points of PI controllers in this thesis. This block has various options for the optimization algorithm such as Nelder-Mead simplex algorithm, Genetic algorithm, etc. From these, nonlinear simplex method of Nelder-Mead is used as the optimization technique in this thesis [40].

For the optimization algorithm, formulation of objective function is very important. This can be done by taking the errors between the reference and actual values of outer loop control parameters as given in equation 3.2. Then this OF is fed to the optimization block in PSCAD/EMTDC to obtain the optimized parameters. The selection of this OF is based on to reduce the error and obtain the actual value close to the reference value [3].

$$OF = \int ((V_{dc} - V_{dc,ref})^2 + (Q_{A,ref} - Q_A)^2 + (Q_{B,ref} - Q_B)^2 + (P_{B,ref} - P_B)^2) \quad (3.2)$$

This objective function has four objectives, i.e. to reduce the error between dc side voltage at the dc bus at VSC\_A, active power at the VSC\_B and reactive powers at both converters. By giving weights to each objective, one can emphasise more on individual sub-objective. In this case, weights are selected to be equal for all objectives giving equal importance to all parts of the objective function. Implementation of the objective function in PSCAD/EMTDC is shown in the Figure 3-6.

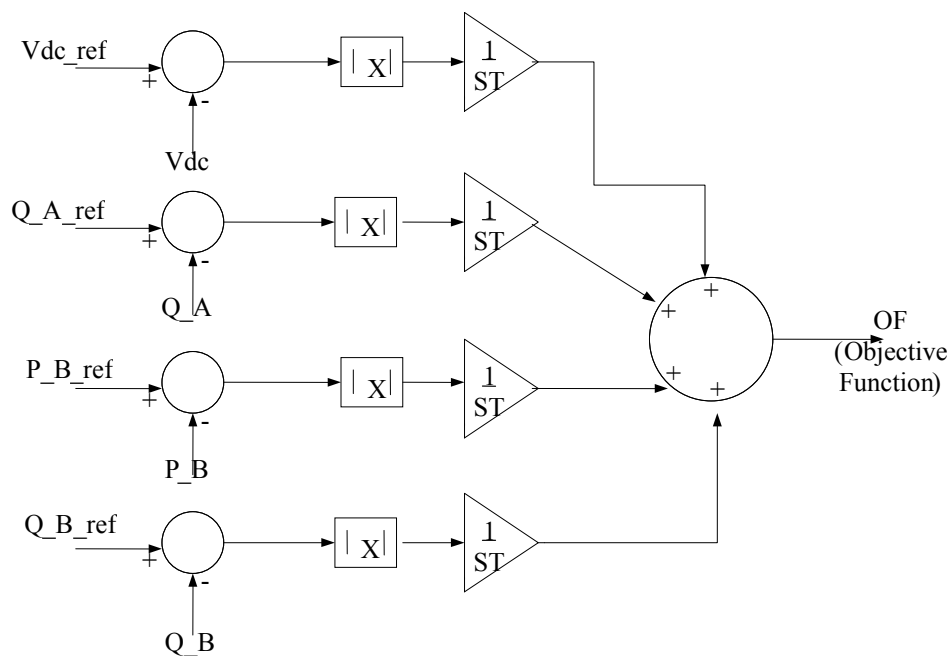


Figure 3-6 : Implementation of the objective function

Then this objective function is fed to the optimization block in the PSCAD/EMTDC as shown in the Figure 3-7. The gains of this diagram are the initial values of the pi controller parameters.

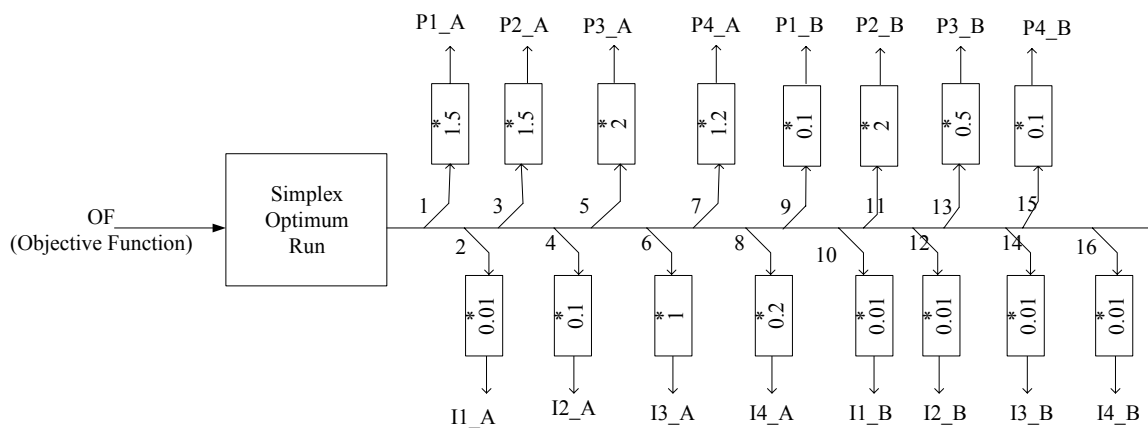


Figure 3-7: Block diagram of Optimization system

Table 2 : Initial values and optimized values of the PI controller parameters of Control system of VSC-A

Parameter	Initial value	Optimized value
P1 (Proportional gain of PI controller 1)	1.5	1.3405
I1 (Integral gain of PI controller 1)	0.01	0.0169
P2 (Proportional gain of PI controller 2)	1.2	1.3221
I2 (Integral gain of PI controller 2)	0.1	1.6761
P3 (Proportional gain of PI controller 3)	2	4.3171
I3 (Integral gain of PI controller 3)	1	2.8471
P4 (Proportional gain of PI controller 4)	1.2	1.7301
I4 (Integral gain of PI controller 4)	0.2	0.4516

Table 3 : Initial values and optimized values of the PI controller parameters of Control system of VSC-B

Parameter	Initial value	Optimized value
P1 (Proportional gain of PI controller 1)	0.1	0.0061
I1 (Integral gain of PI controller 1)	0.01	0.0005
P2 (Proportional gain of PI controller 2)	2	18.5123
I2 (Integral gain of PI controller 2)	0.01	0.0007
P3 (Proportional gain of PI controller 3)	0.5	0.5504
I3 (Integral gain of PI controller 3)	0.01	0.0033
P4 (Proportional gain of PI controller 4)	0.1	0.0187
I4 (Integral gain of PI controller 4)	0.01	0.0005

Table 2 and 3 shows the initial and optimized values of the VSC controllers' parameters, i.e. the PI controller values. The termination criterion is selected to be the objective function value less than 0.1. It took 1128 simulation runs to converge to these values. Total duration of run time is over 12 hours.

This objective function has four parts. One can select one of these objectives and can run the optimization for that objective and can find the corresponding PI controller values. Also each part of this objective function corresponds to 2 PI controllers, i.e. 4 parameters. It is possible to form objective functions for each of these PI controllers and perform the optimization for each of that and tune the PI controllers. For this scheme, it is required to perform the simulation 16 times with each run may have hundred of iterations. Following table summarizes this fact for few cases.

Table 4 : Number of simulation runs and time duration for various parts of Objective Function

Case	No: of simulation runs	Time duration (hrs)
Single PI controller (PI controller 1 at VSC_A)	476	4
Two PI controllers (Q_A control mode at VSC_A)	624	6
All PI controllers (Objective function as in (3.2))	1128	11

As can be seen from the table, when only one PI controller is tuned, it took around 4 hrs while for the whole case it took around 11 hours. If each individual PI controller is tuned separately, it may take days to perform the simulations. This is not practical when the number of PI controllers is high. Also if the system is still developing, it may take a long time to model the system accurately in this way. Another reason for doing optimization with the overall objective function is that even though the sub objectives are optimized properly, it may not ensure the optimized performance of the complete system as adding up of individual objectives may produce difference results as conditions are now changed. That is why the objective function is formulated as in (3.2) combining all objectives into a single objective function and putting weights to emphasize the important objectives.

### 3.5 Complete System in PSCAD

Complete simulation case modeled in PSCAD/EMTDC can be represented as a block diagram shown in Figure 3-7. VSC-A is based on dc voltage control and reactive power control mode. Hence dc voltage and reactive power measurements are taken and send to the control system. Reactive power and active power measurements are sent to the control system of VSC-B as it is based on active power and reactive power control mode.

As the control strategy is based on vector control, it is required that the d, q and 0 components of current and voltages be available to the control system. So voltage, current and the output of phase lock loop need to be sent to the control systems in both

cases. PWM is modelled inside the control system and the generated gate signals are transferred back to the converter.

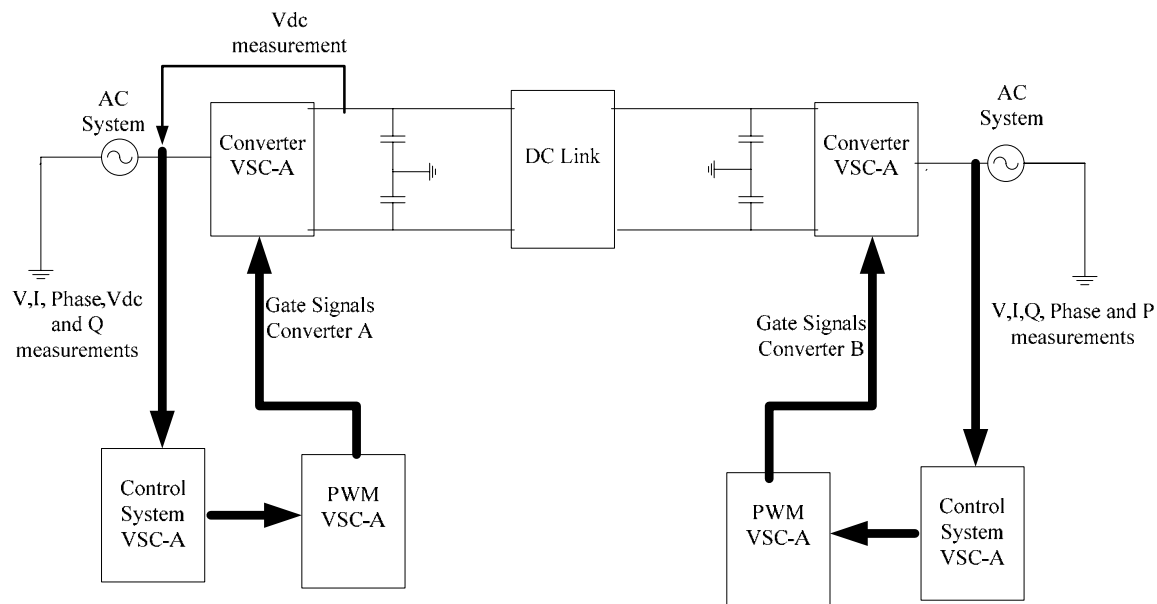


Figure 3-8 : Complete system in block diagram form

### 3.6 Simulation Results

DC side voltage, reactive power at the VSC\_A, active power and reactive power at VSC\_B are varied as below to test the system. These dynamic variations cause excitation of the control system and hence initiate dynamic variations will show as a result. The conformity of the quality of the variation to the specified objective will be measured and captured in the objective function defined earlier.

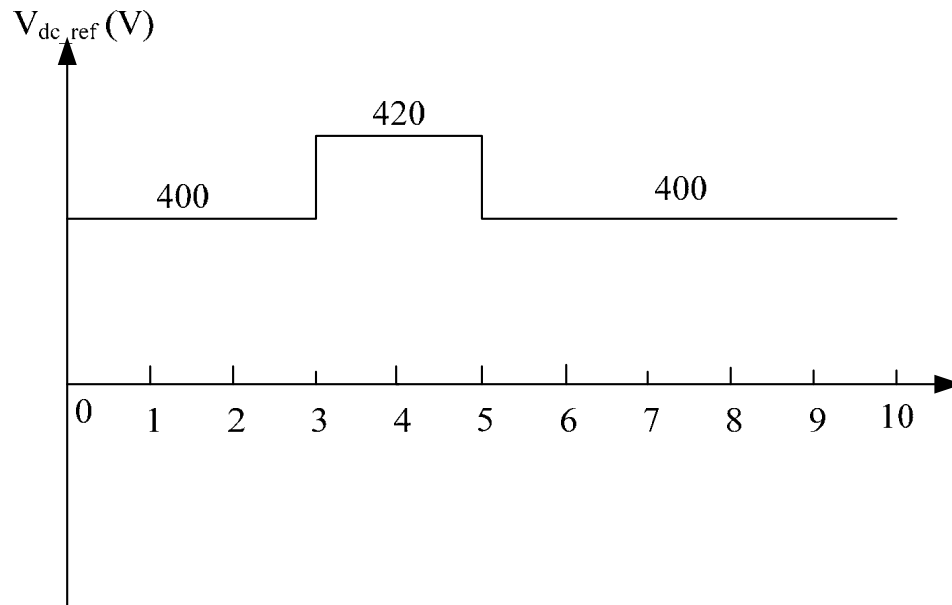
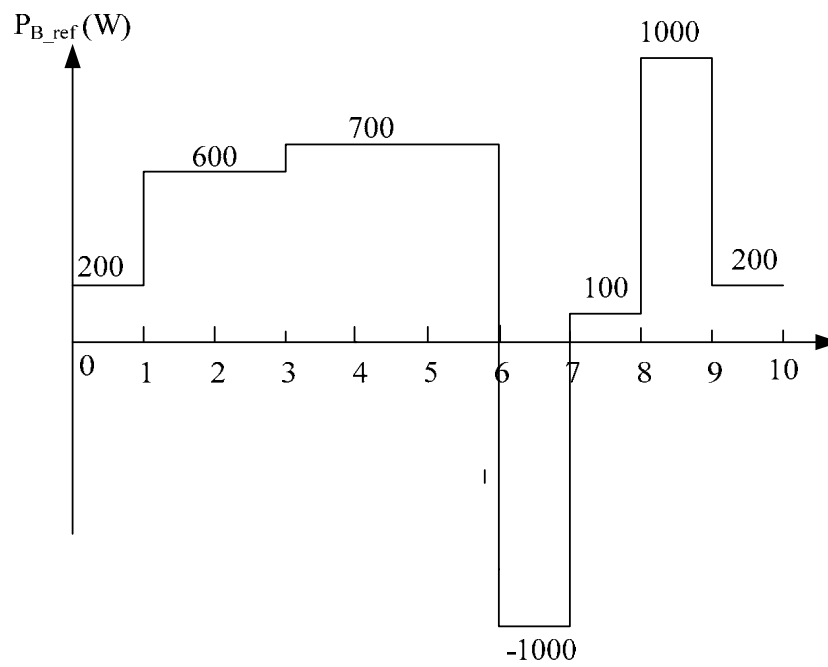
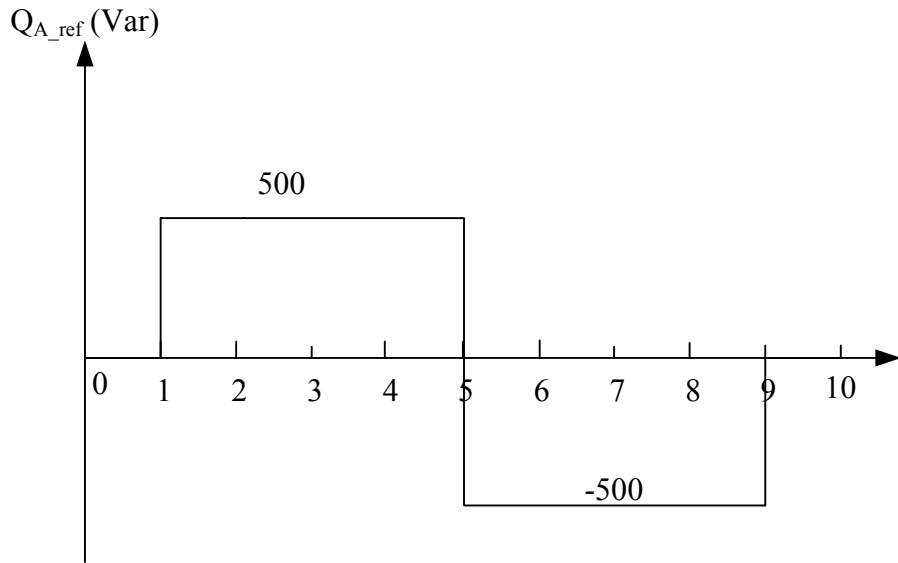
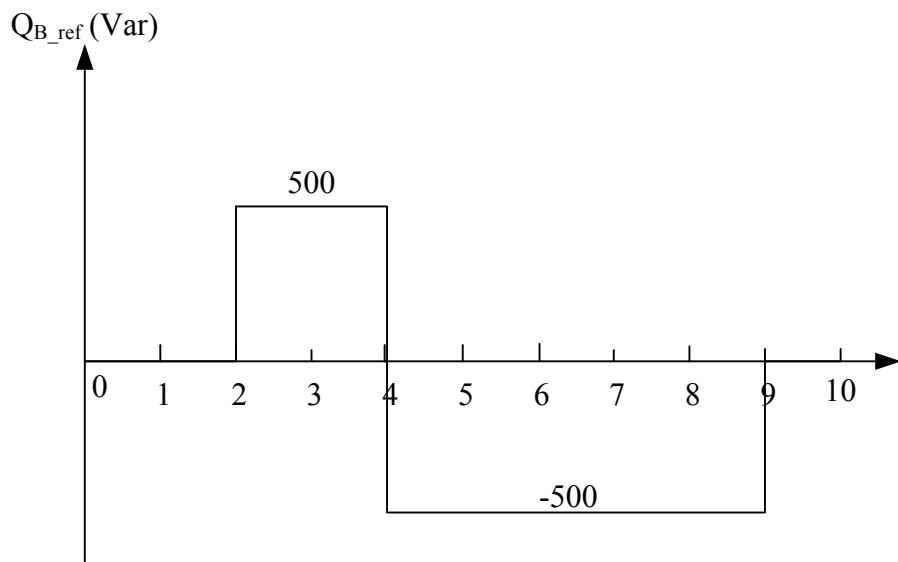


Figure 3-9 : Variation of Vdc

Figure 3-10: Variation of  $P_B$

Figure 3-11 : Variation of  $Q_A$ Figure 3-12 : Variation of  $Q_B$

Simulation results for P,Q, and  $V_{dc}$  for both converters are shown below for before and after the optimization.

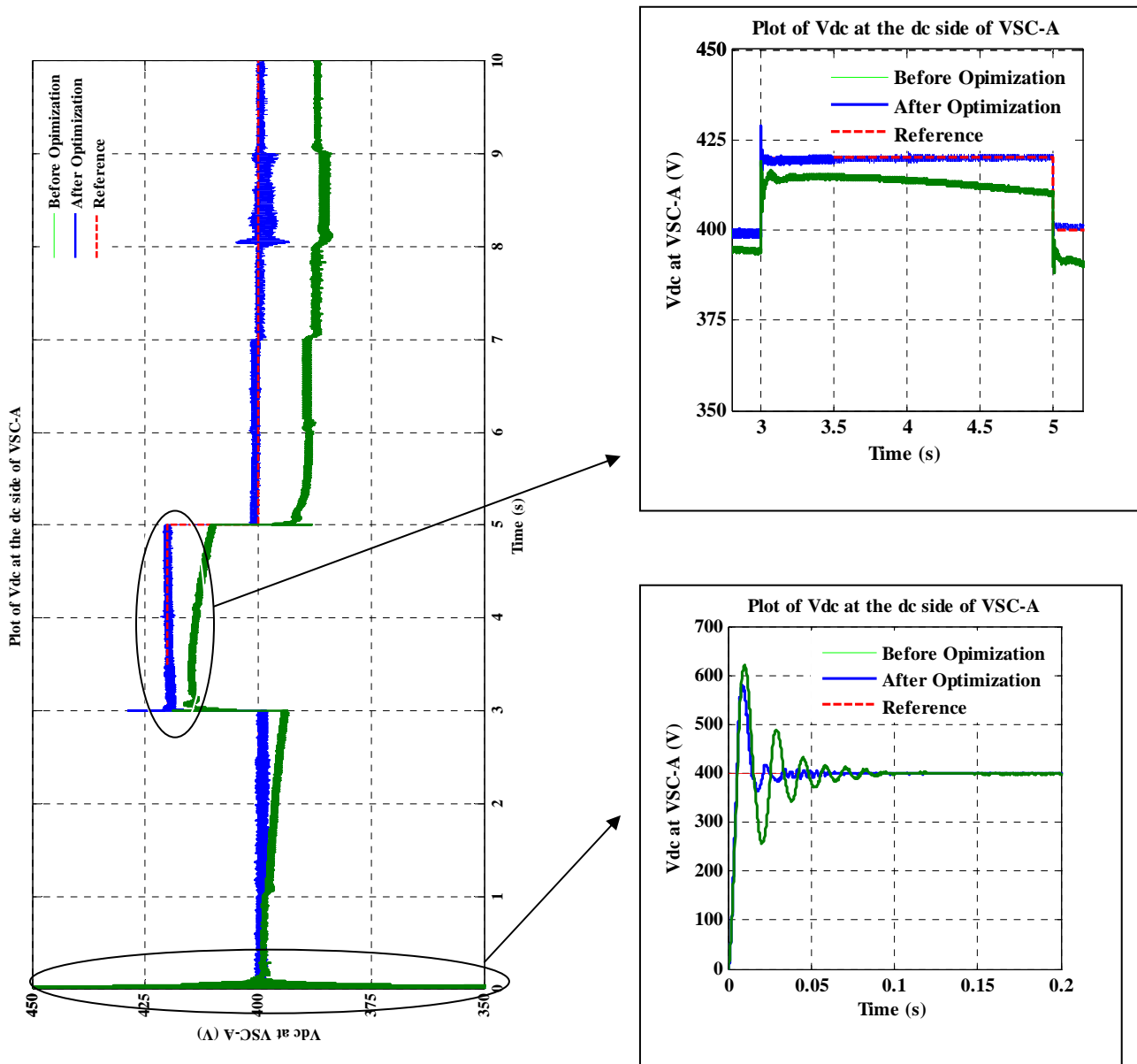


Figure 3-13:  $V_{dc}$  at dc side of VSC-A

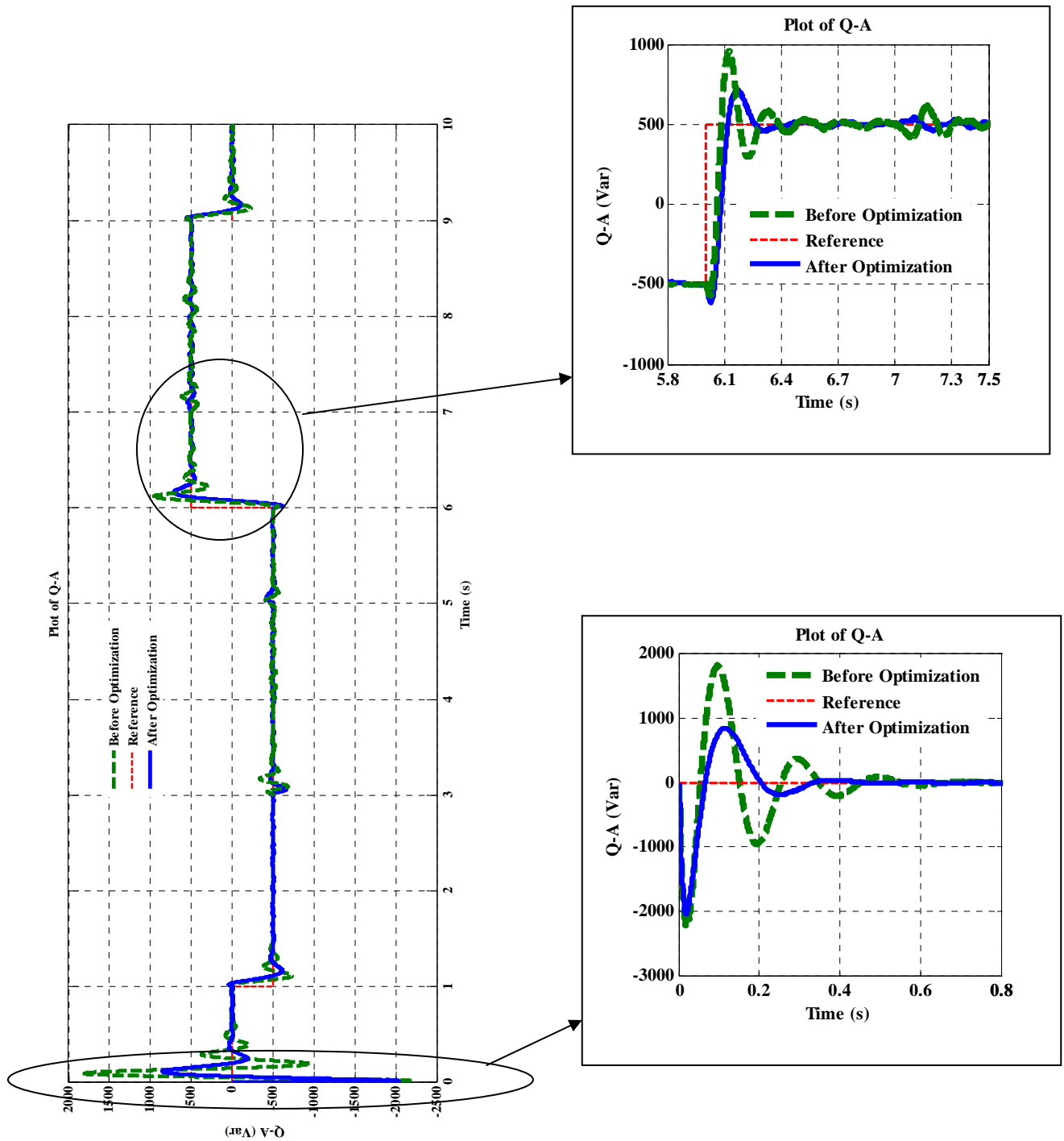


Figure 3-14: Reactive power (Q) at VSC-A

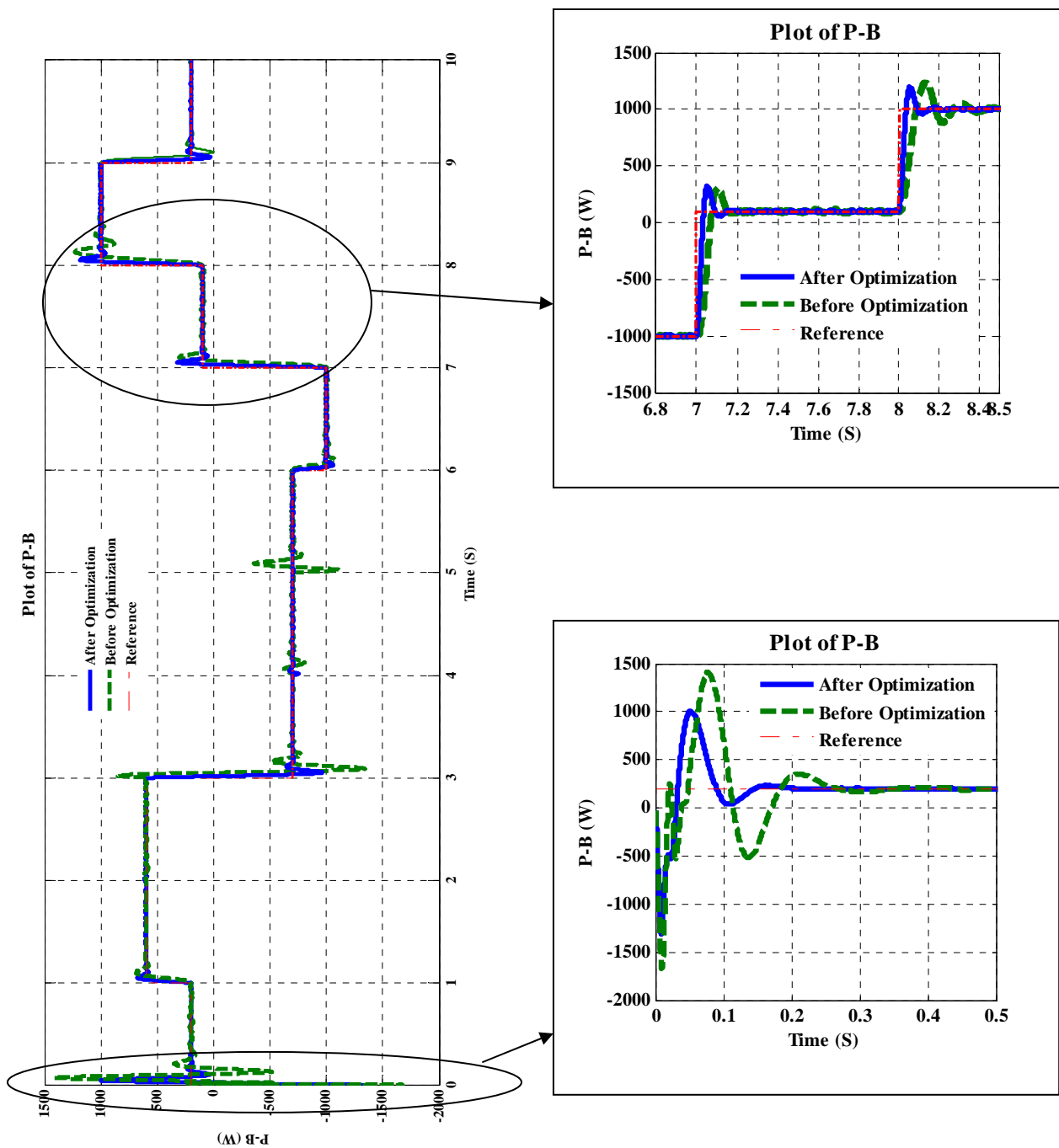


Figure 3-15: Active Power (P) at VSC-B

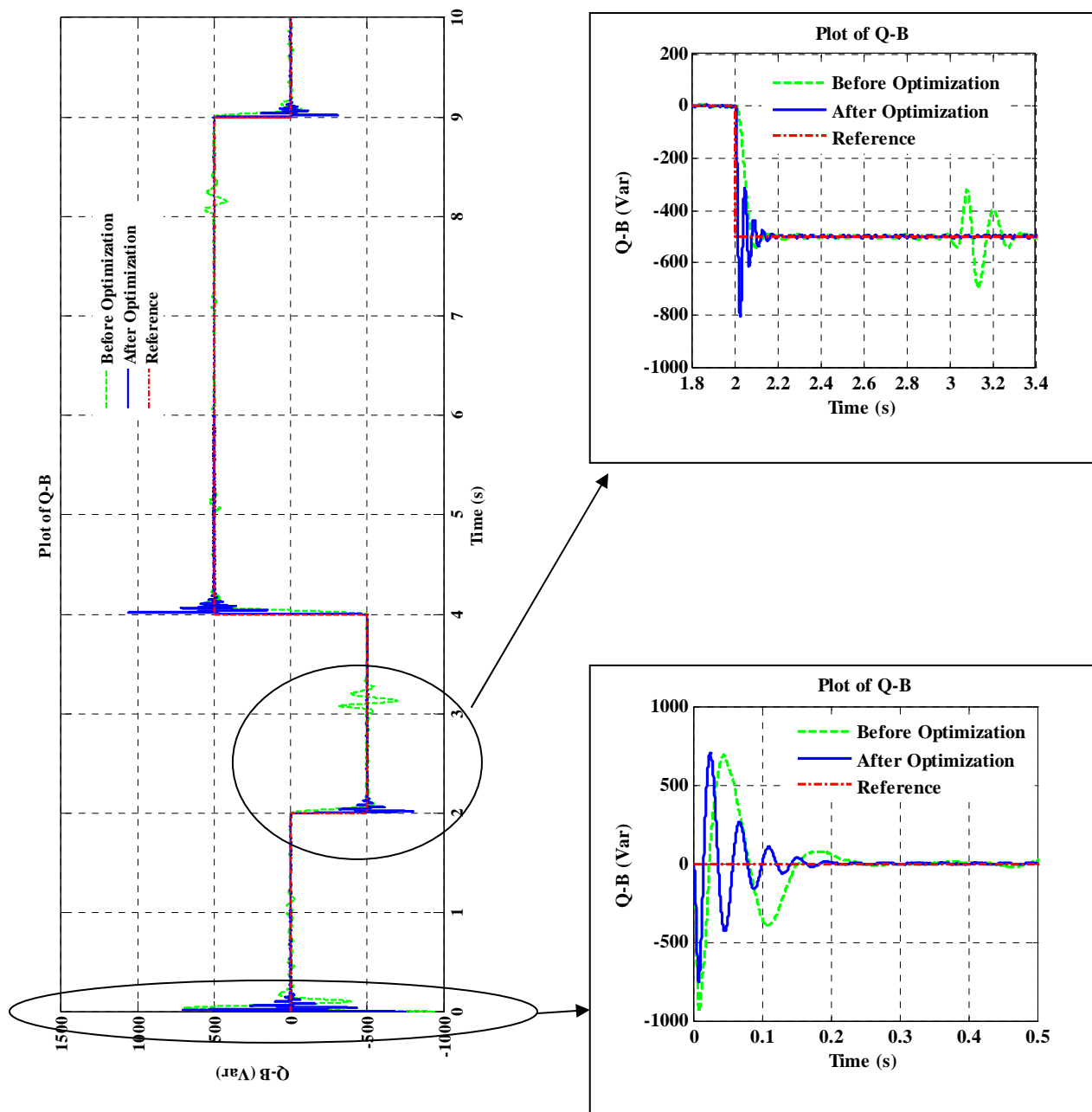


Figure 3-16: Reactive power (Q) at VSC-B

Optimization of the controller parameters has provided a better response as can be seen with before and after optimization graphs. Before the optimization  $V_{dc}$  has a significant steady state error, which is reduced with the optimization results. Before optimization  $Q_A$  plot contains a far higher overshoot and settling time than the optimized case. Also the graphs of  $P_B$  and  $Q_B$  in the optimized case gave a good response when compared with the non optimized situation. These observations at selected time values can be tabularized as below.

Table 5 : Average steady state error % of  $V_{dc}$

Time (s)	t= 3-5 s	t=5-10s
Before Optimization	$((420-415)/420)\% = 1.19\%$	$((395-400)/400)\% = 1.25\%$
After Optimization	$((420-418)/420)\% = 0.476\%$	$((398-400)/400)\% = 0.5\%$

Table 6 : Overshoot of  $Q_A$

Time (s)	Initial	t= 1 s	t= 6s
Before Optimization	1850	-750	950
After Optimization	850	-600	700

Table 7 : Overshoot of  $P_B$

Time (s)	Initial	t= 3 s
Before Optimization	1400	-1350
After Optimization	1000	-900

As depicted in tables, steady state error of  $V_{dc}$  has reduced about 0.7 % while overshoot of  $P_B$  and  $Q_A$  reduced significantly. In the  $Q_B$  plot, variations can be seen when the operating point of the active power at VSC\_B ( $P_B$ ) is changed, before the optimization. These variations disappear with the use of optimized parameter values.

Under the analysis described in Section 2.3, the converter is modelled in a state space representation with three state variables,  $i_d$ ,  $i_q$  and  $V_{dc}$ .  $V_{dc}$  at the right hand side of the converter is shown in Figure 3-12.  $i_d$  and  $i_q$  in both converters are shown below. They show a stable operation around all operating points.

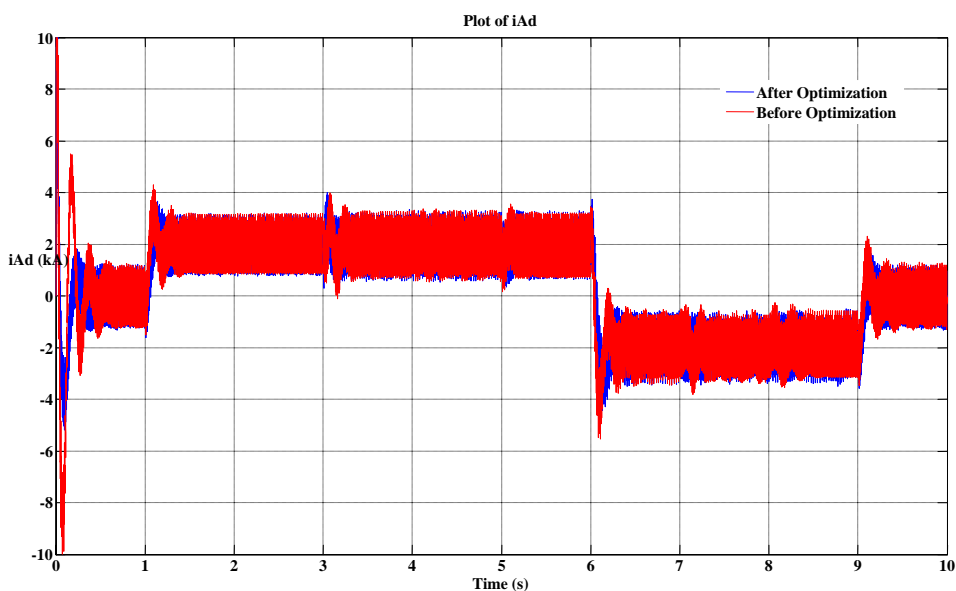
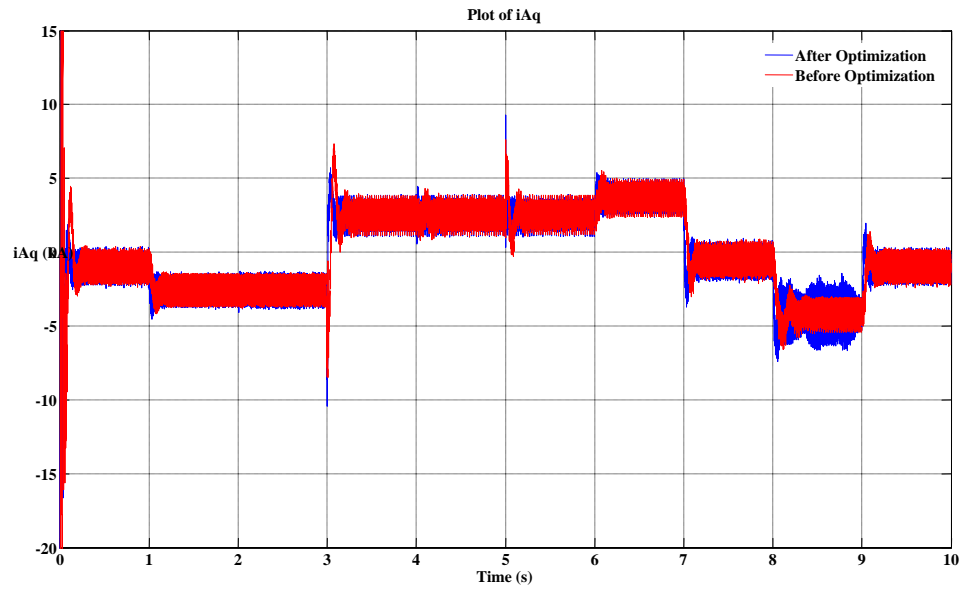
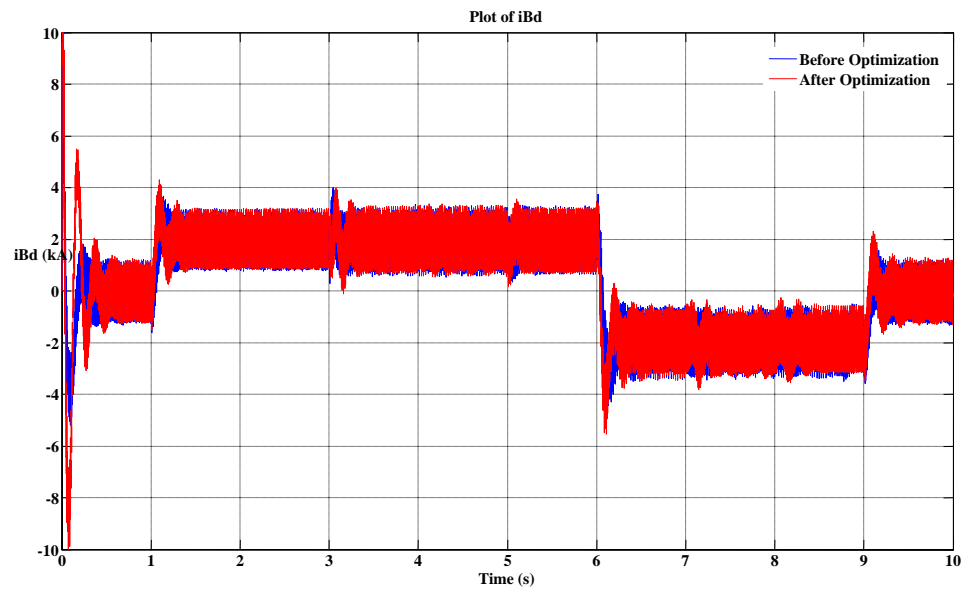


Figure 3-17 : Plot of  $i_d$  at the VSC\_A

Figure 3-18 : Plot of  $i_q$  at the VSC\_AFigure 3-19: Plot of  $i_d$  at the VSC\_B

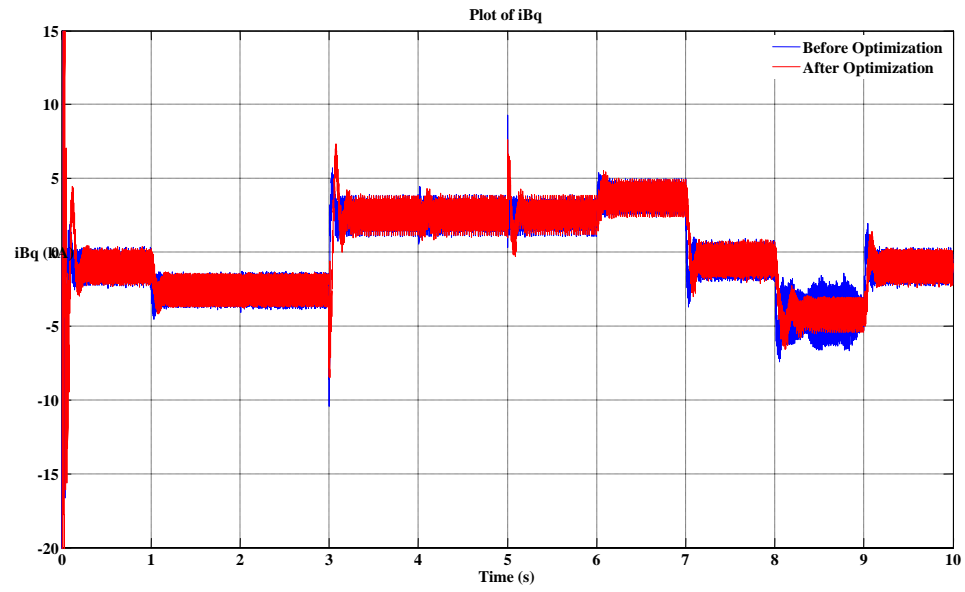


Figure 3-20 : Plot of  $i_q$  at the VSC\_B

## Chapter 4

# Co-Simulation of the Test Case

With the increase in the complexity of the modern power systems, it is often required that more than a single simulation platform be used to study those systems. Some simulation platforms are focused more on detailed models that are required to do the transients studies while others focus more on less detailed models, which can be used in studies like load flow analysis. Platforms having detailed models may be restricted to number of nodes due to the complexity of the components [1]. Availability of functions for performing specialized analyzes is another reason why a specific tool might be favoured for a given study [1].

Even though modern simulation tools come with their own library components for most of the components present in the power systems, users may need to do specific computations which may not include in these components. In such a case user may need to use another tool to perform his/her task [1].

In some cases, hardware needs to be used in conjunction with simulator softwares. Some hardware platforms allow the user to use commercially available software; for ex-

ample dspace platform allows the user to work in MATLAB/SIMULINK environment [22]. In these situations, co-simulation can be used to get the work done.

Based on these facts, it can be concluded that one may need to use more than one platform to perform a given simulation. This can be done by using co-simulation, i.e. modelling the system in more than one platform, each suitable for specific purposes and to interface those platforms using a suitable communication mechanism [1].

In this thesis to perform the co-simulation, PSCAD and MATLAB/SIMULINK is selected. Modelling of the back-to-back VSC transmission system in PSCAD is described under Chapter 3. Since the final target of this work is to investigate a complete design cycle of a back-to-back VSC transmission system, MATLAB/SIMULINK is selected as the other simulation tool as it supports specific tool boxes, which can be used with specific hardware platforms such as dspace that enables the easy prototyping of the actual system to complete the design cycle.

PSCAD and MATLAB/SIMULINK can be interfaced using the commands available in the PSCAD. PSCAD has a command name “SIMULINK\_INT”, which enables the interfacing between PSCAD and SIMULINK. This interfacing scheme however proved problematic in handling initial conditions and as such was abandoned.

Alternatively use of an intermediate MATLAB m-file is proposed. The purpose of this m-file is described in Section 4.2.1. This serves as medium between PSCAD and the SIMULINK models. Interfacing between PSCAD and MATLAB is done by the command “MLAB\_INT” in PSCAD [5]. This forms a multiple interfacing method and can be categorized under chain type interfacing.

## 4.1 Electrical System in PSCAD/EMTDC

The electrical system or the power circuit of the back-to-back VSC system was modelled in PSCAD/EMTDC. This system is similar to the system described in Section 3.1 except only the voltage, current and phase measurements are done in PSCAD. Active power and reactive power calculations are done inside the SIMULINK model.

## 4.2 Control System in MATLAB/SIMULINK

The measurements from the PSCAD model are transferred to the SIMULINK model through an intermediate MATLAB m-file. The control system is the same as the system described in section 3.2 except it is now modeled in SIMULINK. Power measurements required for the control system are done using the power measurements block in SIMULINK.

### 4.2.1 Role of the Intermediate m-file

When the system is interfaced, PSCAD transfers its data to SIMULINK at every time step, or at regularly sampled frequency and receives the output of the SIMULINK file for generation of data for the next time step. In this thesis, communication between PSCAD and MALAB/SIMULINK is done at every time step. As can be seen from the simulation results in chapter 3, parameters have dynamic variations when the operating points are changed. If the communication is done only at sampled frequency, these dynamics may

not be presented clearly and may cause wrong functioning of the system modelled in SIMULINK. Hence communication at every time step is used.

The control system contains a few Proportional-Integral controllers which have integrators inside. Integrator equation is given by the following formula [41].

$$y(t) = \int_{t_0}^t x(\lambda) d\lambda \quad (4.1)$$

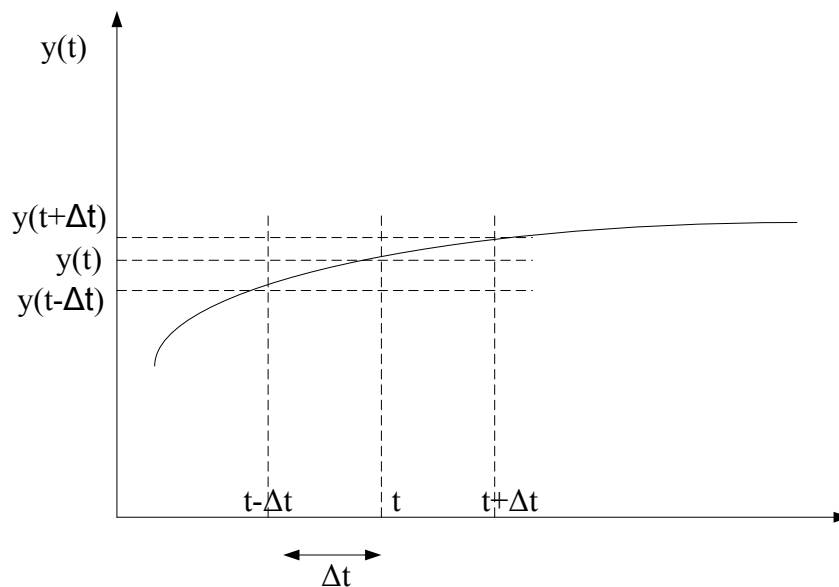


Figure 4-1 : Graphical representation of the Integration

Integration finds the area under the function curve during integration time interval and can be explained using the Figure 4-1. Function  $y(t)$  can be sampled using small time step of  $\Delta t$ . During this time interval,  $y(t)$  can be considered as a straight line. So the integration is equal to the area under the trapezoid. To estimate the area, it is required the history term  $y(t-\Delta t)$ , i.e. the function value at the previous time step,  $t-\Delta t$ .

This implies that initial states are required to obtain the proper value from the integration function. So one has to feed the initial values every time the pi controllers in the

SIMULINK are called. When PSCAD calls SIMULINK it is considered as a new simulation run in the SIMULINK. Therefore it is required to have a mechanism to store the final states of the integrators for the next time step in SIMULINK (or MATLAB) as PSCAD and SIMULINK exchange data in every time step of the PSCAD simulation.

This is the purpose of the MATLAB m-file that handles the communication between the two platforms. First it receives the data coming from the PSCAD and puts them into an array which includes all measurements and the initial states of the integrators. In the first time step, integrator initial states are kept as zero. Then the m-file calls the corresponding SIMULINK file where the control systems are modelled. After the simulation completes in SIMULINK for that time step, the m-file receives the generated output and final states of the integrators and stores them for use as the initial step for the next time step. Finally it transfers the output data of the SIMULINK file (gate signals of the two converters) back to the PSCAD. This process continues until the PSCAD run completes.

This whole communication process can be represented using the block diagram as shown in Figure 4-2.

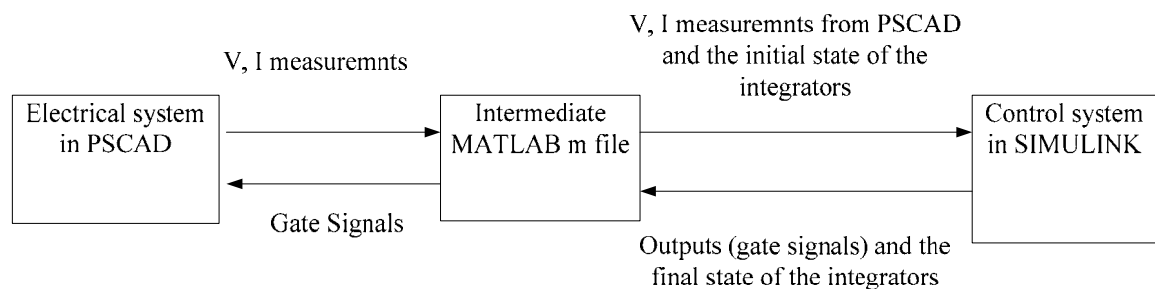


Figure 4-2 : Communication between PSCAD and MATLAB/SIMULINK

## 4.2.2 SIMULINK Control System

The control system is modelled exactly the same as the system in PSCAD using the components available in SIMULINK. Necessary settings have to be done in the simulation parameter dialog boxes to save the integrators' final states which are needed by the m-file for the purpose described earlier. Power measurements required for the control system are done using the power measurements block in SIMULINK. This system takes the voltages, currents and phases of the two AC systems and generates the gate signals of the two converters as the outputs. Sinusoidal pulse width modulation technique similar to the case in PSCAD is used as the modulation technique in generating gate signals.

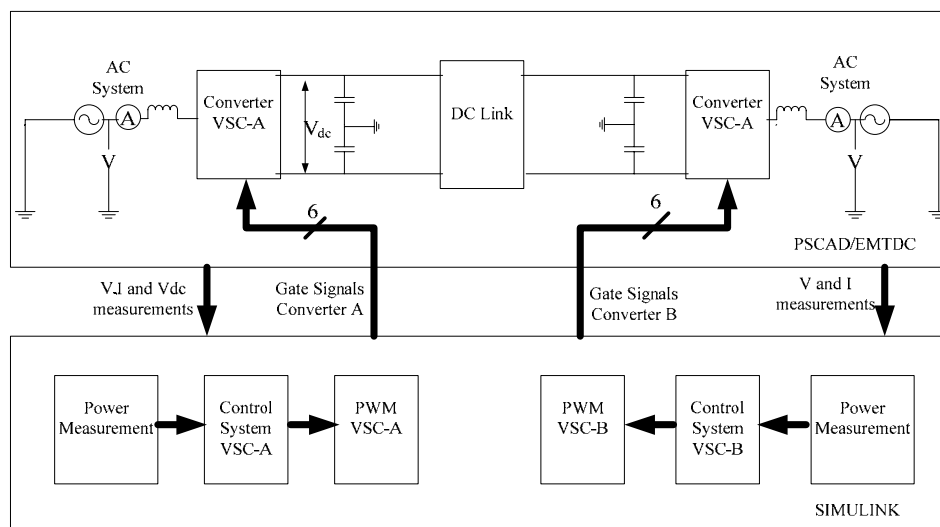


Figure 4-3: Interaction between PSCAD and SIMULINK

The interfacing between the two platforms can be modelled as in Figure 4-3 in block diagram form. Measurements, taken from the electrical system modelled in PSCAD, are transferred to the SIMULINK through MATLAB interface. Based on these inputs, control system in the SIMULINK generated the gate signals which are transferred back to the PSCAD via the same MATLAB interface.

### 4.2.3 Interfacing to MATLAB/SIMULINK

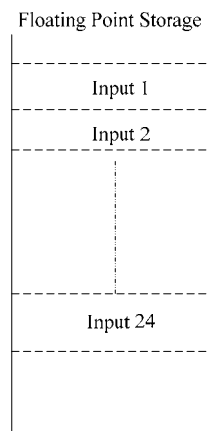
The electrical system described in section 3.1 is modeled in PSCAD while the control system described under section 3.2 is modeled in SIMULINK. An intermediate MATLAB editor file is used to achieve the interface between these two. Interfacing is achieved by defining a new user defined component inside the PSCAD and calling MATLAB from it. The memory allocation has to be done for the parameters that are exchanged between two programs. PSCAD sends measurements of voltage, current and phase as input to the SIMULINK control system through MATLAB. Therefore these data need to be stored in the separate locations in the arrays of PSCAD. In this case, “floating point” array type is used as it contains data of floating point numbers. Also PSCAD receives gate signals from MATLAB and they too have to be stored in separate locations for the use in the next time step.

The procedure inside the user defined component can be explained as next. During the first time step, measured voltage, current and phase are stored at separate locations in the floating point array in the PSCAD. Then PSCAD calls MATLAB through the command “MLAB\_INT” which calls the named MATLAB file. Here one has to define the path and name of the MATLAB file correctly. Next these data are transferred to the control system developed in SIMULINK, which generates the corresponding gate signals. These gate signals are transferred back to the PSCAD through the MATLAB file. Once these data are received, PSCAD stores them in the allocated memory location of the array. This process continues until the simulation run is completed. This sequence of events can be illustrated as shown in the Figure 4-4.

Step 1: Declare memory locations

(Input memory locations for three phase voltages, currents, and phases at both converters, active and reactive power measurements at VSC\_B, DC voltage and reactive power measurement at VSC\_B and reference values of the controller parameters in the outer loop (24 memory locations). Output memory locations for gate signals of two converters (12 memory locations))

Step 2: Store inputs in corresponding positions



Step 3: Call MATLAB using MLAB\_INT

(This will open the corresponding MATLAB file as listed inside the command)

This has a format as shown below.

MLAB\_INT (“*Path of the file*”, “*Name of the file*”, “*Input array type and size*”, “*Output array type and size*”)

Step 4: Store outputs received from MATLAB in corresponding storage as same as for inputs

Step 5: Increment the memory locations to store the data in the next time step

Figure 4-4 : Sequence of events in PSCAD to MATLAB interface [1]

## 4.3 Interfacing Issues

Many issues may arise when two types of software are interfaced as the platforms of these may change from one to other. As explained in Section 4.3.1, one has to store the final states of integrators for the evaluation of next time step inside MATLAB or SIMULINK. This gives a significant problem when the number of integrators is large as explained next. To overcome this problem, an array of integrator states is defined in the m-file to ensure that each individual integrator can access its initial state correctly.

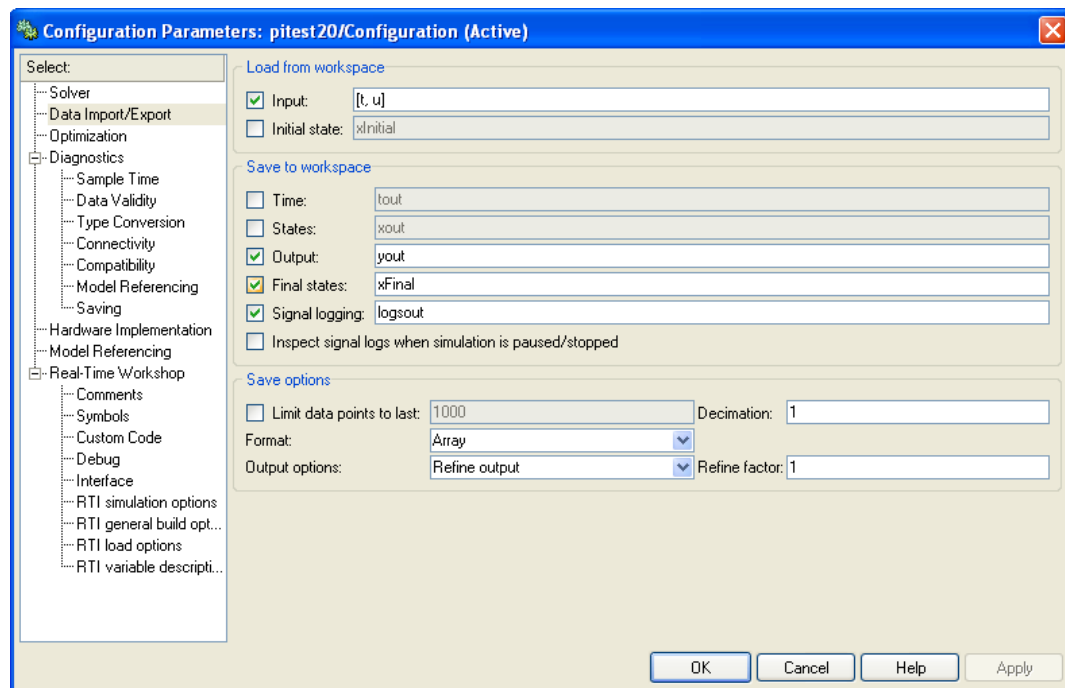


Figure 4-5 : Configuration Parameter Dialog box of SIMULINK

Figure 4-5 represents the configuration parameter dialog box in the SIMULINK. It has several sub sections where “Data Import/Export” sub section is important in this situation. In the data Import/Export section, one has to check the “Input” and “Final states”, if it is intended to transfer states in and from SIMULINK. Integrators final values

at the end of the SIMULINK simulation which are required as initial values for the next time step are stored in an array name “xFinal” under “Final States” in this configuration parameter dialog box [42] and initial state for the next time step is obtained through the array “Input”, which is a two dimension one containing time and input vector having both measurements and integrator initial states. When there is more than one integrator in the SIMULINK file, there is no mechanism to identify the position of a particular integrator state in the array, i.e. it is stored at either position 1 of the array or position 2 or any other position. So trial and error method has to be employed to identify the correct location for a particular integrator state. When the numbers of integrators are large, this is a time consuming task as the interface case requires considerable time for the simulation as discussed below.

The time required to run the simulation increases greatly when the interfacing is done compared with only one platform case. For the original PSCAD case to run the 10s simulation time it only took around one minute. In the same machine with the same simulation time step, interface case took more than 12 hours to run the same duration.

Simulation time step of the PSCAD file has a huge impact on the simulation run time. If the time step is reduced, total simulation time increased rapidly as more data has to be transferred between the two platforms.

If the simulation can be transferred within sampled time step, total simulation run time get reduced as the number of data transfer reduce. However in this case as dynamics are present in the variables at the change of operating points, the data transferred at every time step of the PSCAD simulation is ensured. Also the output from the SIMULINK file

is the gate signals of the two converters. If the data transfer is not achieved at every time step, there is loss of gate signal at during those time steps.

## 4.4 Interfacing Benefits

Despite these problems, co-simulation is important and even necessary in situations where a particular simulation tool is not able to perform a specific function in a part of a project while another tool can be used to perform that operation. Then one can interface these two simulation tools to get the work done [1].

PSCAD/MATLAB interfacing can be used to obtain a more user friendly and attractive visualization way. One can use PSCAD as the simulation tool while MATLAB as the visualisation tool which provide various options to the output object (e.g.: graphs), as well as it provides more attractive look to them. The generated output data can be stored in an array in the PSCAD file. These data can be transferred to the MATLAB file for the visualisation at either interval of simulation time or at the end of the simulation run which result in less time for the whole simulation case.

Co-simulation is valuable when a simulation tool is used in conjunction with hardware. For an example SIMULINK can be used with another software, dSpace which allows easy interface to the hardware. This helps to build prototypes of the real systems reducing cost and time required for testing.

## 4.5 Results Comparison

To test the interface model, same operating points as the case when the complete system modelled in PSCAD is used. Two results sets, i.e. whole system in PSCAD and interface case were compared as below.

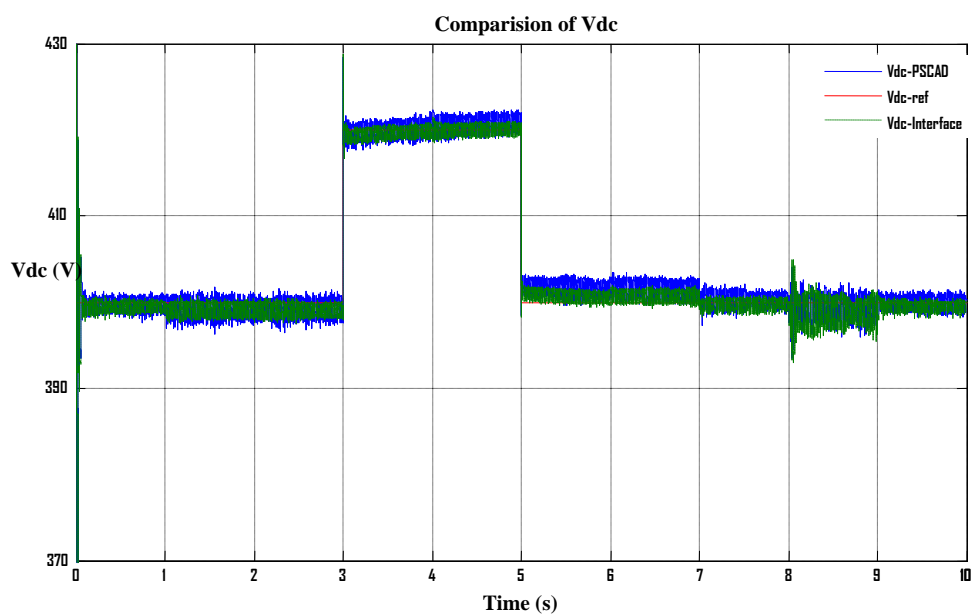


Figure 4-6: Comparison of Vdc

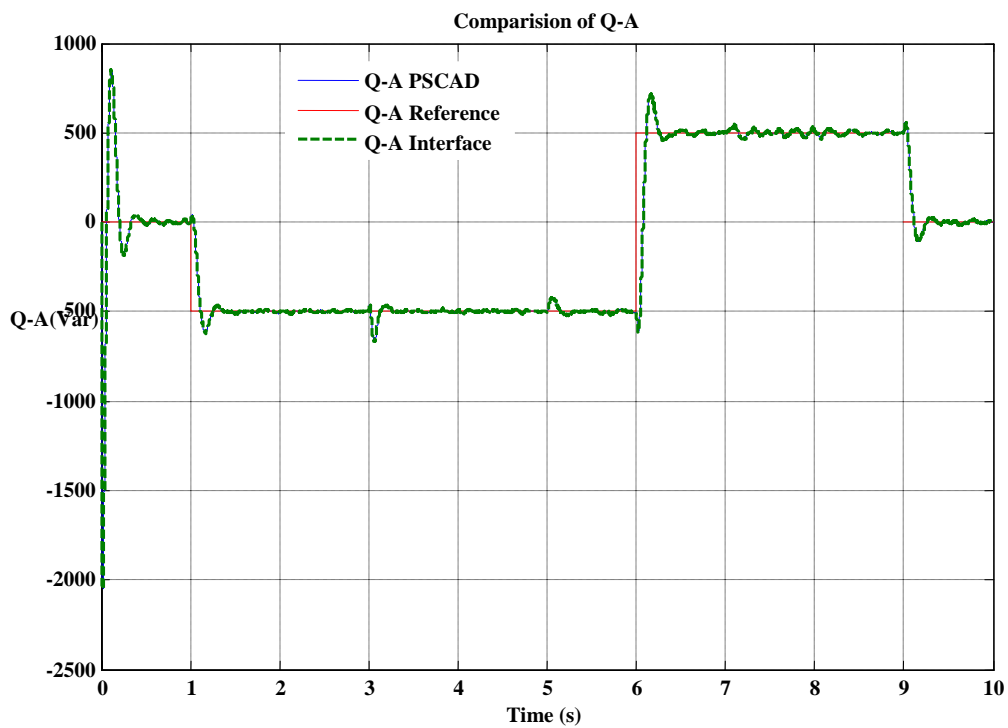


Figure 4-7: Comparison of Q\_A

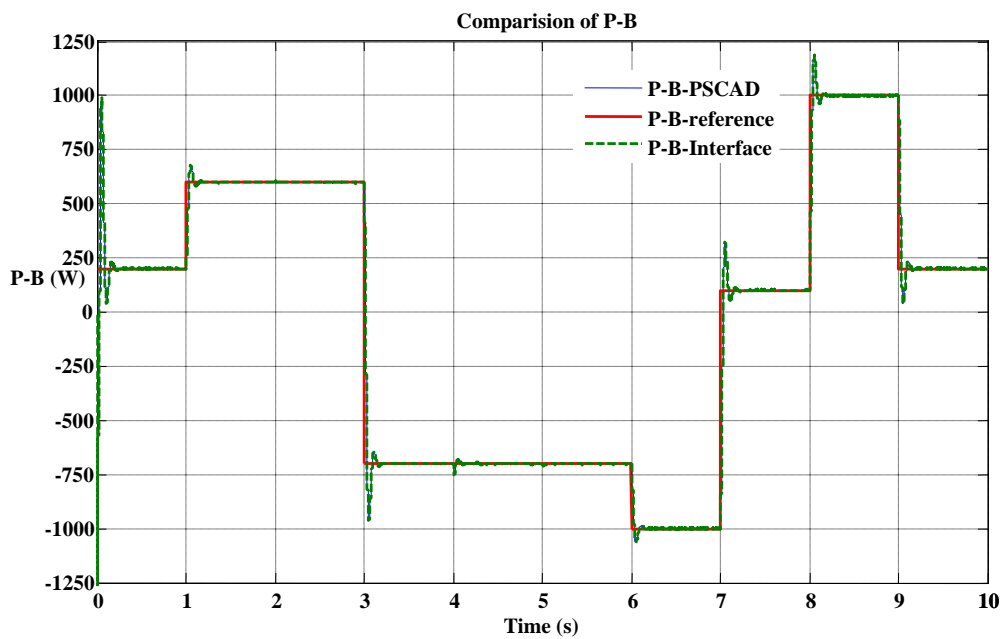


Figure 4-8: Comparison of P\_B

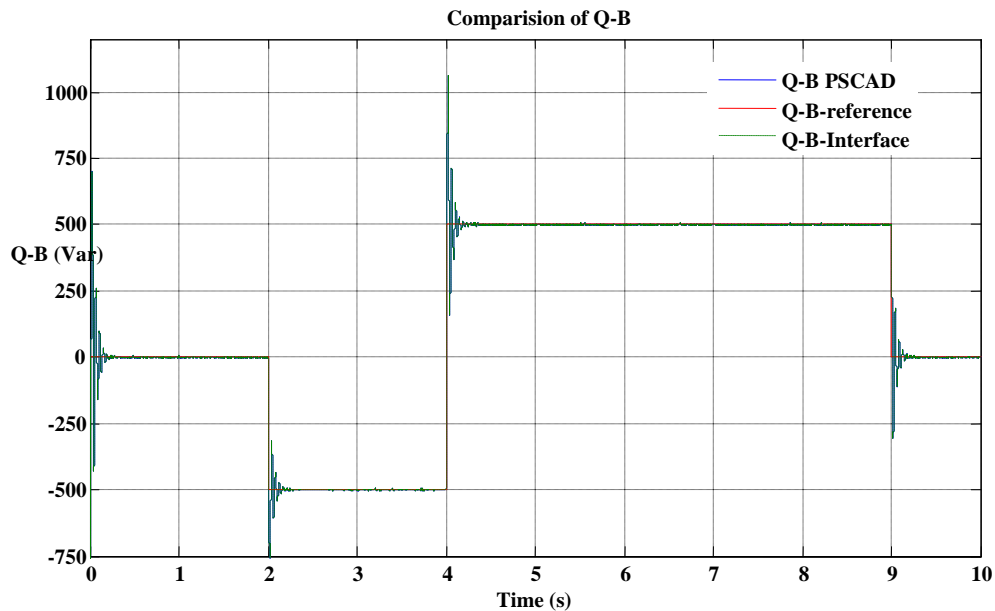


Figure 4-9: Comparison of Q\_B

As can be seen from the graphs, comparison of two cases, i.e. the complete system in PSCAD and the interface case, give identical results. When look at the figure 4-5 to 4-8, the graphs in two cases are on each other proving that they produced exactly the same results. This confirms that the interfaced case work exactly the same as the single platform case. This means the control system modelled in the SIMULINK work exactly the same as the one modelled in PSCAD and the interface between two platforms work fine. In other words, the co-simulation produces the same results as the system only in one platform despite it has issues and benefits as discussed in Sections 4.3 and 4.4.

## Chapter 5

# Conclusions and Future works

### 5.1 Conclusions

This thesis presented a co-simulation of a back-to-back voltage source converter system.

Following things developed under this research.

1. PSCAD simulation model of a back-to-back VSC transmission system was developed. The control system parameters of the model were optimized to achieve an optimized response.
2. The control system of the back-to-back VSC system was modelled in SIMULINK while the rest of the system was modelled in PSCAD.
3. Then interfacing was done to achieve the complete operation of the system through an intermediate MATLAB m-file. Results were compared to verify the two cases produce identical results.

The optimization of the controller parameters gave a better response with less overshoot, less steady state error and less settling time. According to the results obtained in the interfaced case, it can be concluded that the interface model gave the same results as the system only in one simulation program. But the simulation run time in the interface model is far higher than that of the case of the system only in one program. To run the complete simulation model in PSCAD, it takes around one minute with the time step of  $20\mu\text{s}$  for 10s simulation time. With the same time step, same duration, interface model took more than 12 hours to run the simulation in the same computer. There might be other problems that may arise with interfacing as the platform of the interfacing programs may differ. Integrators initial state is such a problem in this case. By using a suitable mechanism, one can eliminate those problems as discussed in chapter 4.

As described earlier, now this model can be used for the hardware implementation stage as the both system give the exact same answer.

## 5.2 Future works

Implementation of the electrical system described in chapters 3 and 4 in the hardware and making the interfacing circuits that are needed to connect the hardware to the control system in SIMULINK. Do the necessary changes to the control system to compatible with dspace platform which use as the interface media between hardware and software.

In this thesis only the balanced cases were considered. Adding of a Clark's transformation to the existing control system to get the sequence components and apply the vec-

tor control to those components makes the system more versatile. In this system any unbalanced situation can be addressed correctly.

Addition of another VSC to the existing dc line makes the system a multi-terminal one. This enables investigation of the system performance in a more complicated situation. Also use of more advanced pulse width modulation techniques, such as space vector modulation and multi-level controlling of VSCs are suggested to improve the performance of the system.

Once the full hardware system is completed, it can be used for testing the system for control application and protection applications.

# Bibliography

- [1] S.Filizadeh, M.Heidari, A.Mehrizi-Sani, J.Jatskevich, J.A. Martinez, “Techniques for Interfacing Electromagnetic Transient Simulation Programs with General Mathematical Tools for IEEE Taskforce on Interfacing Techniques for Simulation Tools,” *IEEE Trans. Power Delivery*, vol.23, no.4, pp, 2610-2622, Oct. 2008.
- [2] H.W. Dommel, “Digital computer solution of electromagnetic transients in single and multiphase networks,” *IEEE Transaction on Power Apparatus and systems*, vol. PAS-88, no. 4. pp 388-399, Apr. 1969.
- [3] A.M. Gole, S. Filizadeh, R.W. Menzies, P.L. Wilson, “Optimization-enabled Electromagnetic Transient Simulation”, *IEEE Transaction on Power Delivery*, vol. 20, no.1, pp. 512-518, January 2005.
- [4] Y. Kuroe, T. Yamamoto, “Computer aided sensitivity-analysis of power electronic control systems and its applications,” in *proc. 1992 IEEE Power Electronic Specialist Conference*, pp. 1293-1300 vol.2.
- [5] Manitoba HVDC Research Centre, *EMTDC User’s Guide*, Winnipeg, MB, Canada, Apr. 2004.
- [6] M. Kezunovic and Q. Chen, “A novel approach for interactive protection system simulation,” *IEEE Trans. Power Delivery*, vol. 12, no.2, pp. 668-674, Apr. 1997.

- 
- [7] L.X. Bui, S. Casoria, G. Moin and J. Reeve, "EMTP TACS-FORTRAN interface development for digital controls modelling," *IEEE Trans, Power Systems*, vol.7, no.1, pp. 314-319, Feb. 1992.
- [8] J. Reeve and S.P. Lane-Smith, "Integration of real-time controls and computer programs for simulation of direct current transmission," *IEEE Trans. Power Delivery* vol.5, no.4, pp.2047-2053, Nov. 1990.
- [9] A.M. Gole, P.Demchenko, D.Kell and G.D.Irwin, "Integrating electromagnetic transient simulation with other design tools," in *proc. 1999 International Conference of Power system Transients (IPST 99)*, Seattle, W.A.
- [10] G.Wild, H. Messener, A. Moosburger, M.H. Xie, A.M. Gole, and D.P. Brandit, "An intergrated simulation and control implementation environment," in *proc. 1997 International conferece Power System Transients (IPST 79)*, Seattle, W.A.
- [11] A.M. Gole and A. Daneshpooy, "Toward Open Systems: A PSCAD/EMTDC to MATLAB interface," in *proc. 1997 International conferece Power System Transients (IPST 79)*, Seattle, W.A.
- [12] M.O. Frauque, Y. Zhang and V. Dinavahi, "Detailed modelling of CIGRE HVDC benchmark system using PSCAD/EMTDC and PSB/SIMULINK," *IEEE Trans. on Power Delivery*, vol. 21, No.1, Jan 2006.
- [13] M.Scezechman, T.Wess, and C.V.Thio, "First benchmark model for HVDC control studies," *Electra*. no. 135, pp 54-73, Apr. 1991
- [14] W.Nye, D.C. Riley, A. Sangiovanni-Vincentelli and A.L. Tits, "DELIGHT.SPICE: An optimized based system for the design of integrated circuits," *IEEE Trans. Computer-Aided Design Integr. Circuits Sys*, vol.7, no.4, pp 501-519, Apr. 1988.

- 
- [15] H. Kragh, F. Blaabjerg, and J.K. Pedersen, "An advanced tool for Optimized design of power electronic circuits," in *Proc. 1998 IEEE Industry Applications Conf.*, vol.2, pp 991-998.
- [16] K. Rigbers, S. Schroder, T. Durbaum, M. Wendt and R. W. De Doncker, "Integrated method for optimization of power electronic circuits," in *Proc. 2004 IEEE Power Electronic Specialist Conf.*, vol.6, pp 4473-4478.
- [17] A.R. Conn, P.K. Coulman, R.A. Haring, G.L. Morill, C. Visweswaraiah, and C.W. Wu, "Jiffy Tune: Circuit Optmization Using time domain sensitivities," *IEEE Trans. Computer-Aided Design Integr. Circuits Sys.*, vol.17, no.12, pp. 1292-1309, Dec. 1998.
- [18] S. Jiang, U.D. Annakage, and A.M. Gole, "Platform for validation of FACTS models," *IEEE Trans. Power Delivery*, vol.21, no.1, pp. 484-491, Jan.2006.
- [19] C.K. Sao, P.W.Lehn, and M.R. Iravani, "A benchmark system for digital time-domain simulation of a pulse-width- modulated STATCOM," *IEEE Trans. Power Delivery*, vol.17, no.4, pp. 113-1120, Oct. 2002.
- [20] N.Kolcio, J.A. Halladay, G.D. Allen, E.N. Fromholtz, "Transient over voltages and over currents on 12.47 kV distribution lines: Computer modelling results," *IEEE Trans. Power Delivery*, vol.8, no.1, pp. 359-366, Jan 1993.
- [21] Q. Bui-Van, G. Beaulieu, H. Hyunh, R. Rosenqvist, "Over voltage studies for the St. Lawrence river 500-kV DC cable crossing," *IEEE Trans. on Power Delivery*, vol.6, no.4, pp 1205-1215 , July 1991.
- [22] dSPACE digital signal processing and Control Engineering GmbH, Germany, *DS 1103 PPC controller board, Installation and Configuration Guide, for release 3.4*, 2008.

- 
- [23] Nikolas Flourebtzou, Vassilios G. Agelidis and Georgios D. Demetriades; “VSC-Based HVDC Power Transmission Systems: An Overview,” *IEEE Trans. on Power Electronics* vol.24, no.3, pp.592-602, March 2009.
- [24] CIGRE, *International Conference of Large High-Voltage Electric Systems*, Study Committee B4, DC Links and Power Electronics, VSC Transmission, pp. 6.1-6.10.
- [25] Cuiqing Du, “The control of VSC-HVDC and its use for large industrial power systems,” Ph.D. dissertation, Dept. Electrical Power Eng., Chalmers University of Technology, GÄoteborg, Sweden 2003
- [26] N. Mohan, T.M. Undeland, and W. P. Robbins, *Power Electronics; Converters, Applications and Design*, Wiley 3<sup>rd</sup> edition, 2003., pp. 200-248.
- [27] M.S. Jamil Asghar, *Power Electronics*, India: Prentice Hall, 2007, pp.299-351.
- [28] L.M. Tolbert, F.Z. Peng “Multi level converters as a utility interface for renewable energy systems,” in *proc. 2000 IEEE Power Engineering Society Summer Meeting*, vol.2, pp. 1271-1274.
- [29] A. Lescinar, R. Marquardt, “An innovative modular multi level converter topology suitable for a wide power range,” in *proc. 2003 IEEE Power Tech Conf.*, vol. 3 pp 6.
- [30] M. Hagiwara, H. Akagi, “PWM control and experiment of modular multi-level converters,” in *proc. 2008 IEEE Power Electronic Specialist Conference (PESC 2008)*, pp 154-161.
- [31] R.L. Hendriks, G.C.Paap, W.L. Kling, “Control of a multi-terminal VSC transmission scheme for connecting offshore wind farms,” in *proc. 2007 Europe’s Wind Energy Conf.*

- 
- [32] J. Morren, S.W.H. de Haan, and J.A. Ferreira, "Model reduction and control of electronic interfaces of voltage dip proof DG units," in *proc. 2004 IEEE Power Engineering Society General Meeting*, vol. 2, pp. 2168-2173.
- [33] B. Mwinoyiwa, Z. Wolanski and B.T. Ooi, "High power switch mode linear amplifiers for flexible AC transmission systems," *IEEE Trans. on Power Delivery*, vol.11, no.4, pp. 1993-1998, Oct 1996
- [34] T. Nagouchi, "Direct Power Control of PWM Converter without power source voltage sensors", *IEEE Trans. Industry Applications*, vol. 34, no. 3, pp. 473-479, June 1998.
- [35] C. Bajracharya, "Control of VSC-HVDC for wind power," M.Sc. dissertation, Norwegian University of Science and Technology, 2008.
- [36] C. Schauder, H. Mehta, "Vector analysis and control of advanced static VAR compensators," in *Proc. 1993 IEE Generation, Transmission and Distribution*, vol. 140, no.4, pp.299-306, July 1993
- [37] C. Du, "VSC-HVDC for industrial power systems," Ph.D. dissertation, Dept. Electrical Power Eng., Chalmers university of technology, G teborg, Sweden 2007
- [38] C. Karawita, U.D. Annakage, "A Hybrid Network Model for Small Signal Stability analysis of Power Systems", *IEEE Trans. on Power Systems*, vol.25, no.1, pp. 443-451, Feb 2010
- [39] Katsuhiko Ogata, *Modern Control Engineering*, India: Prentice-Hall, Fourth Edition, 2002, p. 681-745.
- [40] Edwin K.P. Chong and Stanislaw H. Zak, *An Introduction to Optimization*, Wiley Second edition 2001, pp.287-315,339-454.

- [41] K.A. Strouds, D.J. Booth, *Engineering Mathematics*, New York: Industrial Pres Inc. Fifth Edition 2001, pp. 333-365.
- [42] Mathworks Natick, Massachusetts, U.S.A, *MATLAB/SIMULINK help for Release R2007b*, 2007.

# Appendices

## Appendix 1: Matlab Code for Interfacing PSCAD with MATLAB

```

%=====Matlab program which link PSCAD with Simulink=====
%In this program we transfer [t,u] input vectors to the simulink and
%get Output vectors Y1,...,Y12 from Simulink We need to set input as
%[t,u] and final state as xFinal in Data import/Export in Configuration
%Parameter Dialog box in Simulink

function [y] =
link2sim20(Q_A_ref,Q_A,iAa,V_dc_ref,V_dc,iAb,VAa,VAb,VAc,theta,iAc,dt,t
ime,Q_B_ref,Q_B,iBa,P_B_ref,P_B,iBb,VBa,VBb,VBc,theta_B,iBc)

global t
global u
global xFinal
%Defining the final state of Intergrators which are used as
%initial step for the next time period

%Defining input vector t
t=[time:dt/20:time+dt]';

%Definig input vector u
u=[Q_A_ref*ones(length(t),1) Q_A*ones(length(t),1) zeros(length(t),1)
iAa*ones(length(t),1) zeros(length(t),1) V_dc_ref*ones(length(t),1)
V_dc*ones(length(t),1) zeros(length(t),1) iAb*ones(length(t),1) ze-
ros(length(t),1) VAa*ones(length(t),1) VAb*ones(length(t),1)
VAc*ones(length(t),1) iAc*ones(length(t),1) theta*ones(length(t),1)
time*ones(length(t),1) Q_B_ref*ones(length(t),1) Q_B*ones(length(t),1)
zeros(length(t),1) iBa*ones(length(t),1) zeros(length(t),1)
P_B_ref*ones(length(t),1) P_B*ones(length(t),1) zeros(length(t),1)
iBb*ones(length(t),1) zeros(length(t),1) VBa*ones(length(t),1)
VBb*ones(length(t),1) VBc*ones(length(t),1) iBc*ones(length(t),1) the-
ta_B*ones(length(t),1) time*ones(length(t),1)];

%Using Final states of Intergrators in previous time step as initial
%step in current time step

if time>0.0
    u(:,3)=xFinal(4)*ones(length(t),1);
    u(:,5)=xFinal(2)*ones(length(t),1);
    u(:,8)=xFinal(1)*ones(length(t),1);
    u(:,10)=xFinal(3)*ones(length(t),1);
    u(:,19)=xFinal(8)*ones(length(t),1);
    u(:,21)=xFinal(5)*ones(length(t),1);
    u(:,24)=xFinal(6)*ones(length(t),1);

```

---

```
    u(:,26)=xFinal(7)*ones(length(t),1);
end

%Getting output variables Y1,..., Y12 from Simulink
[T,X,Y1,Y2,Y3,Y4,Y5,Y6,Y7,Y8,Y9,Y10,Y11,Y12] = sim('pitest20',[time
time+dt],simset('SrcWorkspace','current'),[]);

%Assigning output variables obtain from simulink to the vector y to
%pass to PSCAD
y(1) = 10;
y(2) = Y1(length(Y2));
y(3) = Y2(length(Y2));
y(4) = Y3(length(Y3));
y(5) = Y4(length(Y4));
y(6) = Y5(length(Y5));
y(7) = Y6(length(Y6));
y(8) = Y7(length(Y7));
y(9) = Y8(length(Y8));
y(10)= Y9(length(Y9));
y(11)= Y10(length(Y10));
y(12) = Y11(length(Y11));
y(13)= Y12(length(Y12));
```